Detecting patterns of upwelling variability in Eastern Boundary Upwelling Systems with special emphasis on the Benguela region

Amieroh Abrahams

UNIVERSITY of the WESTERN CAPE

RESPICE PROSPICE

DEPARTMENT OF BIODIVERSITY & CONSERVATION BIOLOGY

A thesis submitted in fulfilment of the requirements for the degree of Magister Scientiae in the Department of Biodiversity and Conservation Biology, Faculty of Science, University of the Western Cape

Supervisor: Prof. A.J. Smit
Co supervisor: Dr. Robert Schlegel
September 2020

KEYWORDS

Upwelling

In situ data

Remotely-sensed data

Ocean

Wind

Code:R

Detecting patterns of upwelling variability in EBUS with special emphasis on the Benguela region

A. Abrahams

MSc. Thesis, Department of Biodiversity and Conservation Biology, University of the Western Cape.

Coastal upwelling is one of the most important oceanographic processes relating to biodiversity at local and global spatial scales. To better understand how changes in upwelling trends may occur in the face of ongoing anthropogenically induced climate change it is important to quantify historical trends in climatic factors responsible for enabling coastal upwelling. However, a paucity of knowledge relating to patterns concerning changes in upwelling across the world's oceans over time makes such analyses difficult. Throughout this study I attempted to quantify these patterns by first identifying when upwelling events using a novel method for predicting the behaviours of coastal upwelling systems over time. By using remotely sensed SST data of differing resolutions as well as several wind variables I was able to identify and quantify upwelling signals at several distances away from the coastline of various upwelling systems. Using this novel method of determining upwelling, I then compared upwelling patterns within all Eastern Boundary Upwelling Systems (EBUS) over a period of 37 years, with the assumption that climate change was likely to have driven variable wind patterns leading to a more intense upwelling over time. Overall, upwelling patterns and wind variables did not intensify overtime. This method of identifying upwelling may allow for the development of predicative capabilities to investigate upwelling trends in the future.

DECLARATION

I declare that "**Detecting patterns of upwelling variability in EBUS with special emphasis on the Benguela region**" is my own work, that it has not been submitted for any degree or examination at any university, and that all sources I have used or quoted have been indicated and acknowledged by complete references.

Full name: Amieroh Abrahams **Date:** September 2020

Signature: ....…

ACKNOWLEDGEMENTS

I would like to acknowledge my supervisors. The support provided by them during this process were only surpassed by their insight into the methods allowing the production of this research. Additionally, I would also like to acknowledge all of the sources that contributed to the collection of the *in situ* coastal temperature data used in the second chapter of this thesis. This research was supported by the NRF Grant number SFH180604339745.

PREFACE

This Master's thesis covers the research I have performed over the last two years. This printed body of work is static in nature, the data science upon which it has been built is not. Much of this work may be found at my GitHub page: https://github.com/AmierohAbrahams/.

LIST OF TABLES

CHAPTER 1

GENERAL INTRODUCTION

1.1. EBUSs and the Benguela upwelling system

Globally, there are four major Eastern Boundary Upwelling Systems (EBUS). These include the Benguela Current off south-western Africa, the Canary Current off north-western Africa together with its northern extension off the Iberian Peninsula of south-western Europe, the Peru-Humboldt Current off western South America, and the California Current off the western continental USA and north-western Mexico (Bakun 1990; Pauly et al., 1995; Bakun et al., 2015). Each of these systems are characterized as vast regions of coastal ocean occurring along the western shores of continents bordering the Pacific and Atlantic Oceans. EBUS are narrow coastal bands that contain upwelled water located on the eastern side of their respective ocean basins. EBUS covers only 1% of the world's ocean surface and is among the most productive regions of the ocean (Pauly et al., 1995). This is due to the systems exposure to coastal upwelling, which is defined as the process whereby cold, nutrient rich, high concentrated CO_2, low pH, and low oxygenated waters are pushed to the surface as a result of alongshore winds interacting with the earth's rotation (Pauly et al., 1995). As consequences of upwelling, diverse marine fauna and flora are able to thrive in these areas due to the abundance of nutrients and favourable temperatures.

The benguela upwelling system (BUS) is unique in that it is bounded at both the equatorward and poleward ends by warm water regimes. These currents are forced locally by the wind stress field off southwest Africa (Nelson et al., 1983; Fennel, 1999). The cold Benguela waters are bound in the south by the warm Agulhas retroflexion region and in the north by the southward flowing Angola current. The flow of the Benguela is often considered to be topographically guided (Nelson et al., 1983; Barange, 1991). The Benguela system is split into northern and southern systems by a zone of intense perennial upwelling activity in Lüderitz within the Namibian region (Shannon, 1986; Cole, 1999). The region surrounding the Benguela experiences a persistent along shore wind. This wind is associated with the St. Helena high pressure system (Guastella, 1992; Schultz, 2010). Continental shelf bathymetry and upwelling favourable winds provide a large-scale upwelling mechanism in the Benguela, whereas local topography and meteorology create an alternating pattern of active and passive upwelling circulations along the coast (Chaigneau et al., 2009; Gutknecht et al., 2013) . Upwelling occurring along the south coast of the Western Cape Province within South Africa, specifically along the coastline is generated by local wind with wind increasing away from the coast (Fennel et al., 1999).

1.2. Upwelling

1.2.1. Atmospheric drivers of upwelling

Overall, EBUS form part of the wind-driven ocean circulation, and their existence is dependent on wind direction and strength (Capet et al., 2004). Wind responsible for coastal upwelling are dependent on preexisting pressure gradients and are caused by alongshore, equator ward winds, which responds to both large scale changes in global circulation, namely to the location and intensity of subtropical anticyclones and associated trade winds and to local processes, those associated with the establishment of thermal low pressure systems over the continents in the warm seasons (García-Reyes et al., 2015; Walker, 2020). These winds are caused by cross-shore atmospheric pressure gradients, and these gradients occur predominantly during heating periods.

Regions surrounding the Benguela EBUS, are dominated by anticyclonic high-pressure cells with quasi-stationary positions, resulting in abundant southerly and south easterly winds (Risien et al., 2004; Hagen et al., 2009). The South Atlantic Ocean High is situated along the west, drawing cool, dry air onto the west of the subcontinent (Van Heerden et al., 1998). Solar heating during summer may result in the development of low-pressure cells, known as heat lows, which are absent during the winter (Tyson et al., 2000). As the anticyclones shift north during winter months, the cold westerlies have a substantial impact on the weather of the southern tip of the South African subcontinent (Van Heerden et al., 1998). The atmospheric temperatures along the coastline are largely influenced by the Benguela Current (Van Heerden et al., 1998). Coastal upwelling in the EBUS are mainly driven by wind patterns that cause offshore Ekman transport that cannot be balanced by the horizontal advection of water (Bakun et al., 2004). Further offshore, the wind stress curl causes upwelling by Ekman pumping. The coastal topography and the climatological winds frame the areas of upwelling (Shannon, 1985; Chavez et al., 2009).

Coastal wind regimes along the California current are also dominated by a large-scale pressure system during the summer season, but are also strongly influenced by local terrain and SSTs in the coastal zone (Perlin et al., 2004; Montecino et al., 2005). Terrain features are responsible for flow intensification downwind (Perlin et al., 2010; Perlin et al., 2011). Compounding these wind variations are mesoscale boundary layer effects generated by air–sea interaction with coastal upwelling (Perlin et al., 2010). The intensity of these mesoscale phenomena, spatial extents, and effects on the coastal ocean circulation, however, show some uncertainty and variability in the coastal zone, where coastal topography, the diurnal cycle, and the underlying sea surface temperature (SST) field complicate the analysis (Dorman et al., 2000; Haack et al., 2008).

Overall, Ekman transport forced by equatorward upwelling-favourable winds has been long accepted as the main driver of the greatest eastern coastal upwelling systems (Sverdrup, 1939), where during summer, when SST are warm, upwelling can be observed as a local temperature drop (Gurova et al., 2013), with a typical time series of upwelling ranging from a few days to a few weeks.

1.2.2. Upwelling dynamics

Natural climate variability can be defined as a phenomenon that reoccur at different temporal periods, and is often defined as an influencer on significant trends with EBUS (Rossi, 2010; Walker, 2020). These reoccurring phenomena are often accompanied by reoccurring climatic conditions but the magnitude of the occurrence changes each time. One of the most common example of natural climate variability is El Niño-Southern Oscillation (ENSO). During ENSO, the Walker Cell Circulation is weakened or reversed, resulting in a multitude of teleconnections that have global impacts. Walker Cell Circulation serves as the climatic median for wind direction and the distribution of SST (Rasmusson et al., 1982; Lau, 1997; Rahmstorf, 2002). Commonly, easterly trade winds along both sides of the equator create divergent Ekman Transport that instigates upwelling in the central Pacific Ocean, creating cold SST along the equator (Rasmusson et al., 1982; Scoccimarro et al., 2011). During ENSO, the Trade winds are weakened or reversed, and as a result, central Pacific upwelling is turned into downwelling, creating a warm layer of SST (Klein et al., 1999; Wang et al., 2000; Beaufort et al., 2001).

EBUS have common properties (Blanco, 2001), where under "normal" conditions, the main transport carries cold, well-oxygenated water from high towards low latitudes. The well-known Pacific El Niño (EN) is manifest as an episodic warming of coastal waters off Peru. Warming of the equatorial Pacific is related to major shifts in the Walker circulation (Southern Oscillation) in the atmosphere, ENSO (Bjerknes, 1969). The ENSO caused marked changes in precipitation and wind patterns in the South-East Atlantic (Bakun, 1996; Shannon et al., 1996).

The Humboldt Current (Peru-Chile) and California Current, systems are both directly impacted from EN and La Niña (LN) (i.e. the warm and cold phases of the ENSO cycle) (Halpern, 2002; Arntz et al., 2006; Vargas et al., 2007). The Canary Current however is a special case in that it does not have an oxygen minimum zone (OMZ) (Arístegui et al., 2009; Pelegrí, 2015). OMZ is mainly affected by warm and cold phases of the ENSO. During EN, intra-seasonal Equatorial Kelvin Waves (IEKW) are generated by wind anomalies in the Equatorial Pacific region (Kessler et al., 1995). They propagate eastward and reach the western coasts of the Americas (Gushchina et al., 2012). There, they trigger coastal trapped waves (CTWs) which propagate poleward and impact the vertical structure of physical and biogeochemical variables alongshore off Peru (Echevin et al., 2014; Graco et al., 2017) and Chile (Ulloa et al., 2001). The water column thus becomes oxygenated during EN and a deeper oxycline (>100 m) is observed, while during LN (e.g., 1999–2000), a shallower oxycline is described (Morales et al., 1999).

Coastal upwelling within the Humboldt current exhibits strong interannual variability forced by the ENSO cycle, especially to its warm phase EN (Escribano et al., 2004). Oceanographic changes included the intrusion of oceanic, low-nutrient, and highly oxygenated waters into the coastal areas, with positive SST anomalies. Three main features are present under EN conditions, (i) raise in sea surface temperature, (ii) change of water mass distribution toward the coast, and (iii) decrease of primary production. Although upwelling-favourable winds can increase during EN and the depth of the upwelling source waters can remain rather unaffected, the nutrient supply to surface waters often decreases as the result of complex physical processes that involve downwelling and offshore transport, consequently primary production is reduced under such scenarios (Espinoza-Morriberon et al., 2017). The main physical processes connecting ENSO with the northern upwelling region are related to thermocline perturbations and changes in the alongshore currents forced by equatorial kelvin waves (Shaffer et al., 1997).

The Benguela region expresses the Benguela Niños and are less frequent and intense than the Pacific events (Cury et al., 2004; Florenchie et al., 2004). Benguela Niños are defined as anomalous warm events occurring between the southward flowing Angola current and the Benguela upwelling system off south western Africa (Shannon, 1986). The annual southward migration of the Angola Benguela front introduces warm, saline Angolan water into Namibian coastal water. This seasonal migration is associated with the relaxation of the equatorward, upwelling-favourable wind stress (Boyd et al., 1987), while the southward penetration of warm saline water during the Benguela Niño does not seem to be associated with local winds (Stander et al., 1969). Evidently, Benguela Niños are expressed as regions of abnormal, persistent high SST. Many researchers often associate the equatorial interannual variability pattern in the Atlantic to the ENSO phenomenon (Zebiak, 1993; Sutton et al., 2000). Servain (1985) suggested that eastern tropic oceans are governed by remote wind stress effects through equatorial wave dynamics. The Benguela Niño is believed to be associated with large-scale remote changes in the wind patterns. Hence, anomalies in trade winds may result in Kelvin waves that propagate eastward along the equator, inducing a deepening or a lifting of the thermocline. These warm events are also known to impact fisheries and the climate of this region and are also proven to induce unexpected rainfall events and drastically influence fish abundance and distribution (Boyer et al., 2001; Rouault et al., 2003).

In general, regional ocean climate oscillations like the ENSO and Benguela Niño for the Benguela Current System show considerable variability in temperatures (Minobe et al., 1999) and complicated attempts to assess long term trends (Rimbu et al., 2003). However, many of the trends in recent decades might be associated with these oscillations (Barton et al., 2013). Some of these climate oscillations are expected to increase in amplitude or variance with climate change (Timmerman et al., 1999; Sydeman et al., 2013) which would further influence future trends.

1.2.3. Trends

Studies investigating trends in upwelling favourable winds have found mixed results. This was due to small amplitude of uni-directional wind trends relative to amplitudes of seasonal and decadal wind variability, the short duration of time series relative to decadal variability, inconsistencies in data treatment and changes in measurement techniques used to interpolate or reanalyse data (Cardone et al., 1990). Sydeman et al., (2014) find a more accurate pattern of intensifying upwelling favourable winds in the Humboldt and California systems. In the Canary current however, upwelling favourable winds tend to weaken in some regions. Importantly, there is a strong agreement that significant trends in upwelling intensifications are evident at higher latitudes for all EBUS (Alves et al., 2013; Barton et al., 2013; Stocker et al., 2013). Of all EBUS, the most information on this subject is available from the California Current. In the central-northern portion of this system, upwelling winds primarily occur during the warm months of the year, while the seasonal range of pressure gradients in the southern portion of the system is reduced, and upwelling can occur there year-round. Overtime, the timing of upwelling has trended toward later and shorter upwelling seasons in the northern portion of the California System and longer upwelling seasons in the southern portion (Bograd et al., 2009). In contrast, a modelling study on wind stress curl found increased upwelling in the late season in the northern California System (Diffenbaugh et al., 2004).

The changes in trends derived from models may be due to their coarse resolution, which does not adequately represent smaller scale coastal processes such as upwelling (Caabella et al., 2014). Alternatively, this might be due to failing to adequately incorporate factors such as cloud cover or land-ocean pressure gradients which are useful to identify upwelling. Downscaling global models to the coastal domain of EBUS is required to address some of these issues. When incorporating these factors in studies, promising results are obtained (Garreaud at al., 2009).

There is substantial but conflicting evidence on SST trends in EBUS (Rimbu et al., 2003; Belkin, 2009; Garcia-Reyes and Largier 2010). This is because spatio-temporal resolutions of SST capturing various aspects of upwelling processes and trends are unclear by the interannual to multi-decadal variability that result from oceanographic and atmospheric processes (Snyder et al., 2003). Different SST of differing resolutions suggest different trends within EBUS (Rimbu et al., 2003). The coarse resolution of SST datasets often makes it extremely difficult to separate nearshore upwelling related temperatures from regional and EBUS temperatures. These data products are also unable to solve small scale advection or retention within these systems which ultimately show different trends. Lima and Wethey (2012) use high resolution data to show cooling trends for coastal areas in all but the Canary upwelling system. A consistent agreement along all research is that coastal and offshore temperature trends differ. These studies show increasing or decreasing trends in the nearshore SST, compared with increasing trends in the Benguela (Rouault et al., 2010; Santos et al., 2012) and California upwelling systems (Mote et al., 2010). These trends match the trends of increasing upwelling favourable winds (Sydeman et al., 2014). Climate change associated trends in EBUS may be uncertain by the effects of inshore cooling and offshore warming.

The Humboldt Current System is found to be the only EBUS whose SST trends shows a consistent negative linear trend over a time series of 36 years (Baumann et al., 2013; Seabra et al., 2019). The Aguirre et al., (2019) reanalysis of an ensemble of GCMs found increases in summertime upwelling-favourable winds for both the Benguela current system (BCS) and Canary current system (CnCS). For the CnCS. Rykaczewski et al., (2015) found that a majority of models project significant increases in summertime intensity of upwelling; however, both Wang et al., (2015) and Rykaczewski et al., (2015) detected weakening in upwelling for the lowest latitudes of the CnCS.

1.2.4. Climate Change

Climate change as a result of anthropogenic warming is a global concern of both scientific and political importance. As the human population grows, the rate of global warming increases, resulting in profound effects on marine and other ecosystems (Stenseth et al., 2002; Harley et al., 2006; Hoegh et al., 2010). Climbing temperatures cause a host of additional changes to marine systems, such as rising sea levels, increased ocean stratification, decreased sea-ice extent, and altered patterns of ocean circulation and precipitation (Doney et al., 2011). As this warming intensifies, pressure gradients between land and sea increases, resulting in a greater intensity of upwelling winds (Bakun, 1990; 2010; 2015). In rare cases, projected upwelling increases may overcome the countervailing effects of upper-ocean warming and stratification to cause regional cooling (Auad et al., 2006). Mead et al., (2013) found that coastal ecosystems are at high risk as a result of climate change. More recently, Whitfield et al., (2016) confirmed that coastal biodiversity has been observed to be affected by these effects.

While EBUS have long been on the minds of researchers, their reaction to climate change was not completely questioned until 1990 when Andrew Bakun, published his seemingly simple, yet polemic hypothesis (Sydeman et al., 2014; Bakun et al., 2015). Although in Bakun (1990) did not explicitly conclude that the primary productivity of these regions will increase with climate change, it is well understood that the livelihood of pelagic fish is linked to upwelling trends; therefore, in addition to predicting an increase in the rate of upwelling, the Bakun Hypothesis has been extended to postulations that envisage direct benefits for EBUS fisheries (Bakun, 2015).

1.2.5. The Bakun Hypothesis

As previously mentioned, the atmospheric and oceanic mechanisms responsible for upwelling are interdependent and a change in one variable such as wind direction can have an effect on the distant variables. This idea brought about the rationale proposed by the Bakun Hypothesis. There is no doubt that the earth surfaces are warming rapidly as a response to the impact of anthropogenic greenhouse gasses. Over the past three decades, the earth's atmospheric temperature has warmed by 1.2°C (Wycech et al., 2020) and the earth's oceans have warmed by approximately 0.6°C. Although both land and sea surface temperatures are expected to increase, however, lands lower heat capacity will cause it to warm more rapidly than the earth's ocean (Huyer, 1983; Samantha et al., 2019; Zhang et al., 2019; Jakoboski et al., 2020). These differing heat capacities have led to an overall increase in the pressure gradient force occurring between land and sea. Implications of the pressure gradient force directly increase the equatorial wind speeds. As wind speeds accelerate, the rate of Ekman transport increases resulting in a larger amount of surface waters transferred offshore (Huyer, 1983). When coastal surface waters are displaced faster, the rate of coastal upwelling increases (Bakun et al., 2015). Given this, Bakun et al., 2010, proposed that if there was an increase in greenhouse gases, it would cause more heating during the day and more cooling during the night causing the temperature gradient to increase resulting in a strong pressure gradient, ultimately affecting wind patterns and therefore upwelling, imposing uncertainty in future upwelling trends (Bakun et al., 1990).

The hypothesis remains debated throughout the scientific community. Some researchers deny the logic behind this hypothesis – EBUS warm faster than their neighbouring oceans, thus intensifying pre-existing land-sea pressure gradients, however, researchers also question whether the impact of differential heating has on pressure gradient force ultimately drives the intensification of upwelling within these regions (Rykaczewski et al., 2015; Brady et al., 2017). Rykaczewski et al., (2015) suggests that the mechanisms responsible for the intensification of upwelling dependent pressure gradient force is not driven by differential warming but rather intensifications are constrained to the poleward boundaries of the system and its upwelling season.

1.3. Extreme events in the context of upwelling

Extreme events such as marine heatwaves as defined by Hobday et al., (2016) are prolonged discrete anomalously warm water events that can be described by various statistical metrics such as intensity, duration and the count of events within a time series irrespective of its geographical location. An algorithm exists (Schlegel et al., 2018) that finds extreme thermal events within a long-term (> 30 years) daily time series of SST. It does so by finding the occasions when SST exceeds a threshold (the 90th percentile) in the probability distribution of the data based on an 11-day wide moving mean smoother centred on each day-of-the-year at each pixel.

Using the existing knowledge on upwelling and the extreme thermal event algorithm (Schlegel et al., 2018) , it was decided that upwelling signals could be determined in the same way by identifying a threshold when a drop in temperature occurs and by considering wind patterns as well as duration in order to classify an upwelling signal. Metrics of these upwelling signals could then be compared over a long time series to test for upwelling trends.

1.4. Rationale

Coastal upwelling impacts local climates and ecosystems by lowering atmospheric surface temperatures (influencing wind patterns). While the width of upwelling bands only extends 10-30 km, their productive band extends to approximately 100 km. Hence, coastal upwelling serves as a host of nutrients for phytoplankton (Send et al., 1987), creating a region of survival and prosperity for small pelagic fish (Carr, 2001). Given the importance of coastal upwelling; understanding upwelling trends over time and finding an accurate way of identifying upwelling signals are important. By using the extreme event algorithm, we were able to identify signals to date, duration and intensity.

Since EBUS are responsible for over 17% of global fish catch, their response to climate change has become of particular interest to oceanographers and climatologists (Carr, 2001). During summer months, coastal winds are strengthened by the land based thermal low-pressure system, generally located east of permanent but seasonally migrating oceanic high pressure systems (Huyer, 1983; Seager et al., 2003; Montecino et al., 2009), with the biological productivity in EBUS being mainly as a result of warm seasonal upwelling, this study is important to test for variation in the duration, frequency and intensity of upwelling specifically during summer months.

1.4.1. Predictions/Hypotheses

We predict that intensified upwelling-favourable winds would lead to an increased upwelling rate and duration of these signals. Increased upwelling rate however have significant effects on the surrounding ecosystems and fisheries. Hence, it is important to monitor upwelling trends during the most predominant upwelling period. The importance of coastal upwelling systems is widely recognised, their behaviour is still uncertain (Bakun et al., 2010). Here we hypothesize that upwelling detected at the coastline (0 km) may not be the same signal detected at a distance of 50 km from the coastline given the differences in resolution of SST remotely sensed data. It is also predicted that a higher resolution SST data would likely detect an upwelling signal compared to coarse resolution data. It may therefore be assumed that inaccurate upwelling detection and changes in upwelling trends as a result of climate change will negatively influence these productive zones. In order to investigate upwelling trends the detection and collection of SSTs, wind speed and direction are important. The method used to detect upwelling will represent an extensive body of work and so the application of these results to biotic factors will not be accomplished extensively in this thesis. The important knowledge obtained by this research will branch out into different fields of study, with this it is critical that the work done within this thesis is accessible to other research groups.

CHAPTER 2

UPWELLING SIGNALS: A COMPARISON OF SEA SURFACE TEMPERATURE IN THE BENGUELA

Abstract

The importance of coastal upwelling systems is widely recognised. However, several aspects of the current and future behaviours of these systems remain uncertain, with fluctuations being predicted to occur as a consequence of global increases in temperature, which are hypothesised to affect upwelling-favourable winds. As a result, coastal upwelling is expected to intensify across all Eastern Boundary Upwelling Systems (EBUS). Here, we used sea surface temperature (SST) time series data from five separate data products of varying resolutions to detect and analyse upwelling signals at four sites within the Benguela Upwelling System. Additionally, using wind data, we developed an upwelling index (UI) in order to identify upwelling signals at those regions at varying distances from the coastline. We found that upwelling signals were not uniformly detected across the five data products for each of the four sites and that the durations of those signals were longer when using SST data products with higher spatial resolutions. Moreover, the high-resolution data products were significantly more likely to detect upwelling signals at a distance of 25 km away from the coastline when signals were also detected at shoreline. Our findings promote the viability of SST and wind time series data towards detecting and predicting upwelling signals within coastal upwelling systems. However, our results also highlight the importance of high-resolution data products towards the accuracy of such estimates. This study represents an important step towards the development of a novel method for predicting the behaviours of coastal upwelling systems.

Keywords: Seawater temperature, coastal regions, code: R, upwelling

2.1. Introduction

Sea surface temperature (SST) is regarded as one of the most important ocean-atmosphere systems and is a particularly useful research tool in the scientific fields of meteorology and oceanography (Mesias et al., 2007; Harlass et al., 2015). For over 150 years, SST data has been collected using *in situ* measurement techniques (Rayner et al., 2003)with satellite measurements of SST being available since the 1970s (Reynolds et al., 2013). Furthermore, over the past decade, techniques have been developed to allow the assimulation of different SST datasets from various *in situ* and satellite platforms. These are referred to as the Level-3 and Level-4 high resolution gap-free products. Previous studies demonstrated that satellite-based SST data are less accurate than *in situ* data due to the complexity of the oceanic and atmospheric conditions that need to be accounted for in deriving satellite SST products (Robinson et al., 1984; Brown et al., 1985; Minnett, 1991; Smit et al., 2013). These errors vary both regionally and temporally (Wick et al., 1992). In comparison to *in situ* SST measurements collected from ships, or buoys, a major advantage of satellite SST is their global coverage and near real time availability. SST datasets with a high level of accuracy, spatial completeness and fine-scale resolution are necessary for weather and climate forecasting and are of great importance for reliable climate change monitoring (Reynolds et al., 1995; Smith et al., 1998; Reynolds et al., 2002; Chao et al., 2009)

Long-term SST data have been obtained from two kinds of satellite remote sensors; thermal infrared (TIR) and microwave (MW), which show different weather sensitivity characteristics and accuracies (Li et al., 2013). Infrared remote sensor SST products are available from the 1970's and may have a spatial resolution as fine as approximately a 4 km grid; however, they are unfortunately affected by the presence of clouds and other aerosols in the atmosphere. This is known to result in spatial discontinuity. MW SST products have a lower resolution than infrared SSTs at approximately a 25 km grid, with a much lower accuracy near coastlines (Parinussa et al., 2008; Li et al., 2013). By combining these different types of SST products, it is possible to take advantage of the strengths within both, and each sensor type can help produce an SST dataset with more spatial and temporal coverage and higher resolution.

For many applications, SST data are not used or provided at the full resolution of the sensors but are averaged over defined areas in order to produce a gridded product (Reynolds et al., 2002; Bulgin et al., 2016). Gridding in this way destroys more detailed information and as a result a gridded SST measurement is taken as an estimate of the average SST across a specific grid cell over a certain time period. Spatial sampling uncertainty and temporal averaging is present in gridded products as the full gridded cell is often not being observed as a result of interference due to the presence of clouds or aerosols, as previously mentioned. In existing daily global SST analysis products, typical grid resolution ranges from 0.05°×0.05° to 0.25° ×0.25°, or from approximately 5 to 25 km (e.g., Reynolds et al., 1994; Brasnett, 2008; Donlon et al., 2012). Small scale features can evolve during the course of the day, but the sensor sampling during this time is not dense enough for the sub-daily global analyses at a high spatial resolution (Reynolds et al., 2010; Reynolds et al., 2013). Furthermore, considering that the satellites are passing overhead only once every ~24 hours, therefore, images are only captured at very specific times during the day. It bares mention that sensors can't resolve small-scale features as they continue to evolve over the course of day; the reason being that the sensors are only looking at a restricted portion of the ocean for several minutes at a time; the exception being of-course, geo-stationary satellites like the POES (polar orbiting environmental satellite). To capture these small-scale features in a gridded analysis, it is suggested that the development of an improved analysis would have high resolution at small-scale features in regions of good coverage and lower resolution in areas of poor coverage (Reynolds et al., 2013).

In order to assess the suitability of a range of SST products for coastal application, this study aimed to observe patterns and trends in upwelling signals in the Benguela Upwelling System (BUS) across a range of localities and spatial scales off the South African West Coast. We selected an upwelling system because this physical process provides a strong signal of increasing and decreasing SST that is strongly localised to known centres of upwelling, and which relates to the coastal wind field that drives the offshore advection of water mass. Because upwelling is a well characterised oceanographic process, the resultant fluctuating SST signal should be observed across independent SST products – here we assess blended SST products covering a range of spatial grid resolutions from 0.05°×0.05° to 0.25° ×0.25°. We hypothesized that the higher resolution data should have a better fidelity at detecting these upwelling signals, some of which might only be confined to smaller spatial scales or localised closer to the shore.

The BUS is one of the four major Eastern Boundary Upwelling Systems (EBUS) (Bakun et al., 2015). EBUS are characterised as vast regions of coastal ocean occurring along the western shores of continents bordering the Pacific and Atlantic Oceans (Bakun, 1990; Pauly et al., 1995; Bakun et al., 2010; Bakun et al., 2015). Coastal upwelling associated with EBUS is known to have a large influence on the associated ecosystem's primary productivity, and hence the abundance, diversity, distribution and production of marine organisms at all trophic levels (Bakun et al., 2010; 2015). According to the 'Bakun hypothesis,' an increase in greenhouse gases will result in an increase in day-time warming and night-time cooling and ultimately cause an increase in temperature gradients which will form stronger atmospheric pressure gradients (Bakun, 1990). It should be noted pressure gradients modulate the winds which ultimately affect the intensity and duration of upwelling (Hsieh et al., 1992; Bakun et al., 2010; Lima and Wethey, 2012; Mote et al., 2002). Furthermore, changes in sea surface temperatures indirectly affects coastal communities, and bears considerable, often far-reaching economic impacts as well (Murawski, 1993; Bakun et al., 2010). It is hypothesised that the upwelling signal detected at the coastline is not the same upwelling signal detected at a distance of 50 km away from the coastline by making the assumption that higher resolution data should be able to detect gradients better than the coarser resolution data and that signals are more visible closer to the coastline.

2.2. Methods

2.2.1. Site Selection

The South African coastline exhibits a large variation in seawater temperature and is divided into four bioregions (Mead et al., 2013; Smit et al., 2013). The western region of the coastline is dominated by the Benguela Current forming an Eastern Boundary Upwelling System (EBUS) (Hutchings et al., 2009), which provides a natural laboratory for this study. Annual mean coastal seawater temperatures within this region have a range of 12.3 ± 1.2°C at the Western limit near the Namibian border. Seasonal upwelling is controlled, with intense upwelling occurring throughout the summer months, by south-easterly trade winds and as a result reflects distinct temperature variations representing much lower temperatures within the upwelling cells over a fairly narrow continental shelf found from the Cape Peninsula to Cape Columbine. In order to examine upwelling patterns at different distances from the coastline, several sites from the SACTN dataset (Schlegel et al., 2016; 2017) along the west coast of South Africa (i.e. sites influenced by the Benguela current) were selected. As the main objective of this study was to use a new method of determining and identifying upwelling signals and then to ascertain whether or not the same upwelling signals were detected congruently throughout the various SST products; a study period of four years of data was sufficient in order to compare congruency among the detections between products. Four sites were selected, occurring at different regions in the Benguela system, these include Port Nolloth, Lamberts Bay, Sea Point and Saldanha Bay (**Figure 2.1**).

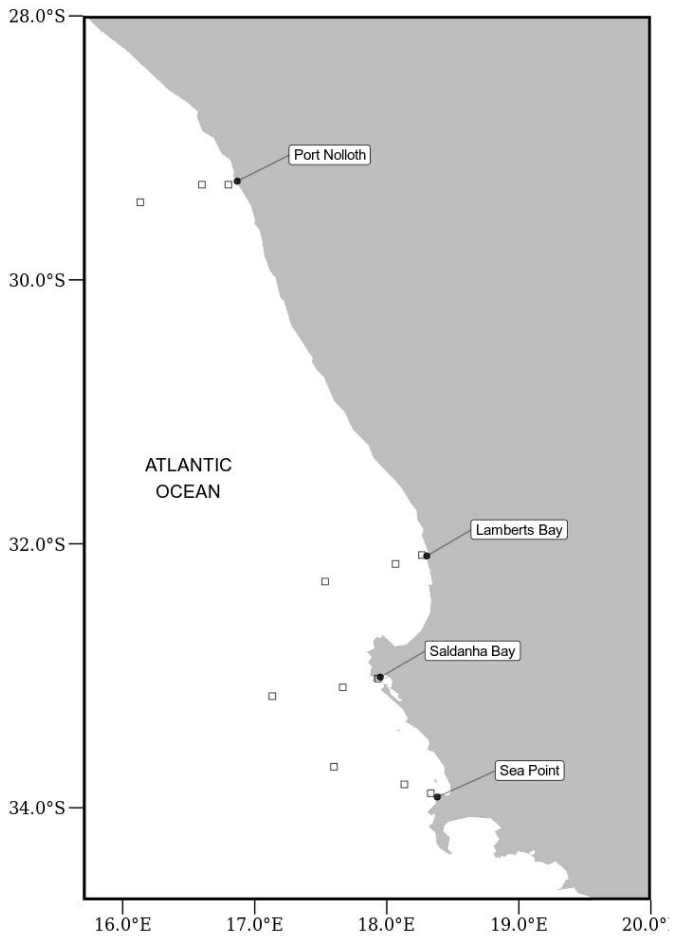

Figure 2.1: A map of the study region along the west coast of South Africa. The black points represent the location of the *in situ* temperatures and the empty boxes show the pixels used along the shore normal transect from the satellite sea surface temperatures (SST) time series. The black boxes are at 0 km, 25 km and 50 km from the coastline.

2.2.2 Datasets

This study uses four Level-4 remotely sensed temperature datasets; compiled by a number of organisations. The AVHRR-only (Advanced Very High-Resolution Radiometer) Optimally-Interpolated Sea Surface Temperature (OISST) dataset has been providing global SSTs for nearly four decades (Reynolds et al., 1994). OISST is a global 0.25° × 0.25° gridded daily SST product that assimilates both remotely sensed and *in situ* sources of data to create a gap free product (Banzon et al., 2016). The second is a version 3.0 Group for High Resolution Sea Surface Temperature (GHRSST) product with a 0.2° × 0.2° global grid resolution constructed by the Canadian Meteorological Center (CMC). It combines infrared satellite SST at numerous points in the time series from the AVHRR, the European Meteorological Operational-A (METOP-A) and Operational-B (METOP-B) platforms, as well as the microwave SST data from the Advanced Microwave Scanning Radiometer 2 in conjunction with *in situ* observations of SST from ships and buoys from the ICOADS program. The Multi-scale Ultra-high Resolution (MUR) Sea Surface Temperature Analysis is produced using satellite instruments with datasets spanning 1 June 2002 to present times. MUR provides SST data at a spatial resolution of 0.01° × 0.01° and is currently among the highest resolution SST datasets available. The final dataset used is the GHRSST analysis produced daily using a multi-scale two-dimensional variational (MS-2DVAR) blending algorithm on a global 0.01° grid known as G1SST. This product uses satellite data from a variety of sensors, such as AVHRR, the Advanced Along Track Scanning Radiometer (AATSR), the Spinning Enhanced Visible and Infrared Imager (SEVIRI), the Moderate Resolution Imaging Spectroradiometer (MODIS), and *in situ* data from drifting and moored buoys. We see that not all products are completely independent as they share the use of AVHRR SST data, but the amount of subsequent blending, the incorporation of other SST data sources, the different blending and interpolation approaches used, and the differing final grid resolutions make them comparable in this study.

Additionally, this study uses the South African Coastal Temperature Network (SACTN) dataset for its source of *in situ* temperature. This dataset consists of coastal seawater temperatures obtained from 129 sites along the South African coastline, measured daily from 1972 until 2017 (Schlegel et al., 2016, Schlegel et al., 2017). Of these, 80 were measured using hand-held thermometers and the remaining 45 were measured using underwater temperature recorders (UTRs). For this analysis, the data were combined and formatted into standardized comma separated values (CSV) files which allowed for a fixed methodology to be used across the entire dataset. Prior to data analysis, all data points exceeding 35°C and/or below 0°C were removed as these were considered irregularities. These data points were then changed to NA (not available) so as to not interfere with analysis.

An advantage to using *in situ* data over satellite data is that they may provide a more accurate representation of the thermal properties closer to the coast, whereas satellite data often fails to accurately capture and represent temperature properties within the same spatial context; the result being *in situ* data can therefore more accurately explain upwelling signals within the coastal inshore environment. Further evidence by Smit et al., (2013) has shown that satellite data collected along the South African coastline may have a warm bias as high as 6°C greater than *in situ* temperatures within the nearshore environment. In order to create a time series of each of the remotely sensed SST data products, shore-normal transects of all Level-4 products were extended at West Coast stations where the *in-situ* data in the SACTN database were available. Time series of SSTs were extracted at 0, 25 and 50 km along these shore-normal transects from the coast shown as black boxes in **Figure 2.1**.

2.2.3 Wind data

Wind data were obtained using a wind instrument called the RM YOUNG Weather Transmitter. This compact instrument provides reliable and accurate measurements of four key meteorological variables. Ultrasonic wind speed and direction, atmospheric pressure, humidity and temperature sensors are carefully integrated into an enclosure optimized for durability, airflow and mitigation of solar radiation effects. Wind was an important variable for this study as wind direction and wind speed have a direct influence on the intensity and duration of upwelling, consequently, wind data collected from 1989-01-01 to present were investigated for their relationship with upwelling at the sites for which SST time series were created. When the instrument collects wind data, the raw files are converted by the logger into a format readable by the metcap program, which draws the graphs and writes the data into excel spread-sheets in which they are stored for later use.

2.2.4 Defining and determining upwelling

In order to detect and analyse upwelling signals at four sites within the Benguela Upwelling System, it was first necessary to define when upwelling was occurring; however, to accomplish this a set of threshold values for identifying when the phenomenon was taking place was required. Given that upwelling is primarily caused by alongshore, equatorward winds, both SST and wind data were used. The wind data were used to inform an upwelling index calculated using the formula presented in the work by Fielding and Davis (1989):

$$upwelling\ index = \mu(\cos\theta - 160)$$

where μ represents the wind speed (m/s), θ represents the wind direction in degrees, and 160 is the orientation of the west coast (Jury 1980). The index relies heavily on wind speed and direction data in order to determine the presence of upwelling and its intensity. The above equation produces a value called the *upwelling index.* An *upwelling index* < 0 represents downwelling whilst an *upwelling index* > 0 represents upwelling (Fielding et al., 1989). When the upwelling index is greater than 0, SSTs usually drop, as expected, suggesting that upwelling is occurring. It was found that the drop in SST that coincided with a positive upwelling index was close to the seasonally varying 25th percentile threshold for SST, so this threshold temperature was used in combination with the *upwelling index* to identify when upwelling may be occurring. With the bottom threshold set for which temperatures may qualify as an upwelling signal it was then necessary to determine the number of consecutive days that must be exceeded for an upwelling signal to qualify as a discrete event. Here it must be noted that upwelling is known to vary on a seasonal basis and may also occur hourly (sub-daily). Therefore, the minimum duration for the classification of an upwelling signal was set as one day. The rationale being that data from the SACTN dataset as well as the satellite remotely sensed SST data are collected only at a daily resolution, preventing a temporally finer definition. With the upwelling index, temperature threshold, and duration for an upwelling signal established, the `detect_event()` function from the **heatwaveR** package (Schlegel et al., 2018) was used to calculate metrics for the upwelling signals. Because upwelling signals were calculated relative to percentile exceedances, rather than an absolute definition such as temperatures below a fixed temperature threshold, upwelling signals could occur any time of the year, however, upwelling was shown to be more dominant during spring and summer months, as expected. This method of determining upwelling signals are unique as it considers both SST and wind pattern, and provides us with a descriptive statistical output of each of the signals detected.

A series of ANOVA tests were used to compare the main effects of the chosen variables on the continuous variable. In this analysis the relationship between the SST products across the various selected study sites was established; factors used to correlate these relationships included duration and the number of signals detected. These analyses sought to test if significant differences occurred between sites and data products. A correlation analysis was constructed to determine if a signal detected at a distance of 0 km from the coastline would be visible at a distance of 25 km from the coastline and, similarly if the same trend could be observed when comparing the 0 to the 50 km offshore regions.

2.3. Results

The durations of upwelling signals detected at each site were not uniformly detected across the five data products (**Figure 2.2**). At both Lamberts Bay and Port Nolloth, the durations of upwelling signals were noticeably lower to those of Saldanha Bay and Sea Point respectively, and appeared to last for a shorter number of days overall. Additionally, signal duration in Lamberts Bay and Port Nolloth both had narrower ranges to those of Saldanha Bay and Sea Point respectively across each of the data products.

Variation of the number of upwelling signals detected across all data products at each site also showed noticeable differences. The median upwelling duration at Lamberts Bay did not exceed 10 days. However, the ranges varied per product with the MUR dataset exhibiting the widest range as well as the maximum duration in comparison to other products. The CMC and SACTN products had relatively similar ranges, but the SACTN dataset had more outliers present. Conversely, Port Nolloth showed no major differences in detected durations between data products. The median duration of signals exceeded 10 days in the G1SST and MUR data products. A slight overlap was present in the overall ranges in the G1SST, MUR and OISST products. Here the OISST and MUR dataset also showed a large variance in maximum duration range.

Saldanha Bay showed differences in durations of signals detected between data products. Here, the OISST and MUR datasets both had comparatively larger medians, maximums, and overall ranges to the CMC and SACTN datasets respectively. In Sea Point the MUR data product represented the widest range, highest maximum and highest median, indicating that it has the greatest fluctuations in duration length. SACTN had a comparatively narrow overall range suggesting a high level of agreement in duration length between events and therefore greater consistency. CMC and OISST datasets were relatively similar but CMC has a lower median.

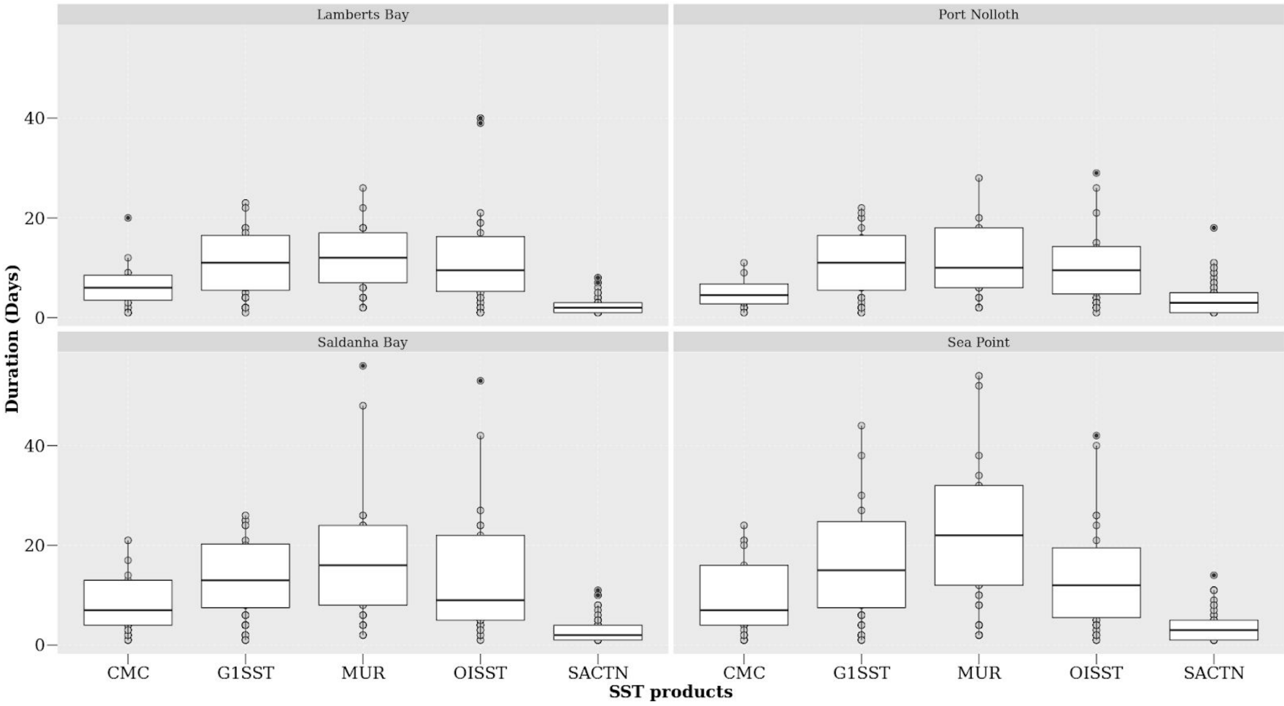

Figure 2.2: The duration for each of the signals detected for the four satellite products and the SACTN *in situ* collected data when upwelling was most dominant during summer months (December, January and February), over a four-year period.

The comparison of the upwelling metrics further revealed that there was an overall significant difference between the durations of upwelling signals collected from the different products (three-way ANOVA: $F = 7.31$, SS = 1111, $p < 0.001$), at the different distances ($F = 4.40$, SS = 223, $p < 0.03$) and across the different sites ($F = 6.34$, SS = 963, $p < 0.001$). The mean intensity of upwelling events also differed between data products ($F = 52.16$, SS = 40.5, $p < 0.05$) and across sites ($F = 41.58$, SS = 32.30, $p < 0.05$), as well as at different distances from the coastline ($F = 265.35$, SS = 68.70, $p < 0.002$) with the most intense signals detected in the MUR and G1SST data products. Similarly, there were also a significant difference between the average cumulative intensity of signals detected across data products ($F = 2.30$, SS = 10604, $p < 0.001$). This same pattern was present between sites ($F = 2.722$, SS = 1294, $p = 0.001$) and also between distances from the coastline ($F = 44.66$, SS = 7078, $p < 0.001$), with the MUR and G1SST data products having the highest cumulative intensity.

Table 2.1: A pairwise correlation of the relationship between the number of signals detected at a distance of 0 km versus a distance of 25 km and between the number of signals at 0 km and 50 km.

Product	Site	0 km vs 25 km	0 km vs 50 km
OISST	Lamberts Bay	0.59	0.14
	Port Nolloth	0.76	0.38
	Saldanha Bay	0.65	0.42
	Sea Point	0.76	0.18
CMC	Lamberts Bay	0.12	0.05
	Port Nolloth	0.66	0.54
	Saldanha Bay	0.44	0.33
	Sea Point	0.69	-0.01
MUR	Lamberts Bay	0.60	0.29
	Port Nolloth	0.74	0.58
	Saldanha Bay	0.52	0.23
	Sea Point	0.63	0.42
G1SST	Lamberts Bay	0.73	0.32
	Port Nolloth	0.66	0.65
	Saldanha Bay	0.28	0.33
	Sea Point	0.57	0.30

Pairwise correlation tests revealed that the likelihood of observing the same upwelling signal detected at 0 km from the coast at 25 km and at 50 km from the coast respectively varied across the individual data products at each of the four sites (**Table 2.1**). However, I found that overall, the chances of observing upwelling signals that were simultaneously detected at 0 km and at 25 km were considerably higher than that of observing those same signals at a distance of 50 km from the coastline. In addition, the chances of detecting upwelling signals at 50 km from the coastline were notably low throughout all pairwise comparisons apart from signals detected at Port Nolloth using the CMC, MUR, and G1SST datasets.

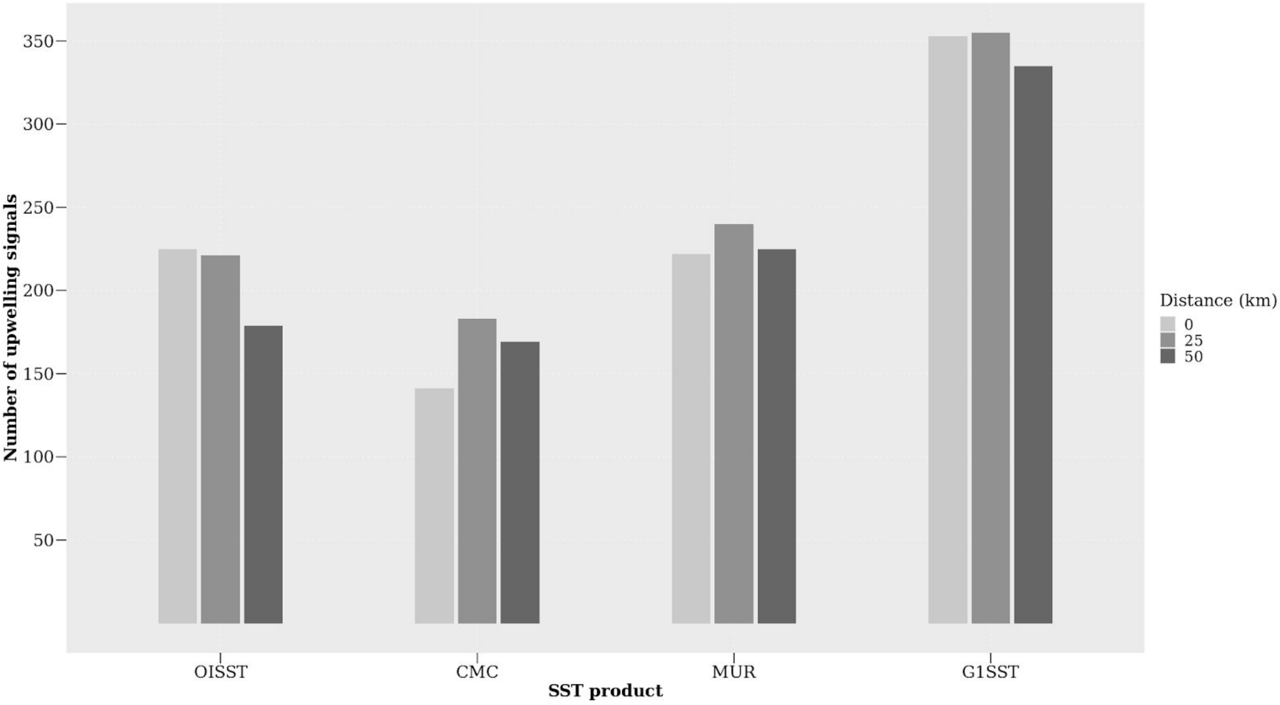

Figure 2.3: The number of the signals detected for the four satellite products since 2011 until 2014.

Although each of the individual data products detected differing numbers of upwelling signals at distances of 0 km, 25 km, and 50 km from the coastline respectively (**Figure 2.3**), these did not differ significantly when taking the distances and data products into account (two-way Chi square test: $\chi^2 = 8.969$, $p = 0.175$, df = 6). Moreover, comparisons of the numbers of upwelling signals across the different distances from the coastline within each dataset showed that there were no significant differences within the CMC ($\chi^2 = 5.566$, $p = 0.062$, df = 2), MUR ($\chi^2 = 0.812$, $p = 0.667$, df = 2), G1SST ($\chi^2 = 0.698$, $p = 0.705$, df = 2) datasets but there was a significant difference within the O1SST dataset ($\chi^2 = 6.234$, $p = 0.044$, df = 2) which had a notably low number of signals detected at 50 km from the coastline. Overall, the G1SST data product detected the most signals, and the CMC dataset detected the fewest.

2.4. Discussion

I report here that upwelling signals detected by the highest resolution data, specifically the MUR data which is collected on a 0.01° grid displayed signals lasting for a longer duration when compared directly to the CMC, G1SST, OISST and SACTN data products. Analysis of the OISST, CMC and SACTN datasets revealed that recorded signals often did not exceed a duration of 10 days. Additionally, this was the same for the higher resolution data products (G1SST and MUR) which also showed a high abundance of signals detected at a duration of less than, or equal to 10 days. Furthermore, it is also evident that the highest number of signals detected were recorded by the MUR and G1SST data products. This may be due to the errors in any satellite Level 4 product, that are a result of accumulation of errors from different sources, as well as the quantification of one component sampling error and thus requires us to focus on this error source alone (Liu et al., 2013).

MUR and G1SST data sources which yield upwelling signals with the longest duration and highest intensity; both rely heavily on satellite data sources whereas the CMC and OISST products are generated from a broader spectrum of data collection methods using multiple sources of satellite and *in situ* collected dataset. As a result, the MUR and G1SST data products are more likely to be affected by contamination from clouds and aerosols (Ricciardulli et al., 2004). Consequently, the durations and intensity of upwelling signals derived from these high-resolution products may be falsely detected at exaggerated lengths. On the other hand, datasets constructed from multiple data sources, particularly from ships and buoys, are inherently more reliable in terms of reducing the frequency of falsely detecting signals. The extended duration and high intensity of upwelling signals detected by MUR and G1SST may be as a result of the microwave frequencies where land surfaces have a higher emissivity (0.9) compared to the ocean (0.4). Microwave observations in the proximity of land are affected by the warm emission of land entering the antenna near-in side-lobes. This warming of the microwave brightness temperatures is a source of errors in the TMI retrievals of coastal waters. Since infrared retrievals are not affected by land emission (if retrieved at least a few kilometres from the coast) (Ricciardulli et al., 2004). However, microwave instruments are able to retrieve SSTs in non-precipitating cloud-covered regions where IR instruments cannot.

It was also found that signals detected at the shoreline are often the same signal detected at the 25 km region. However, when a signal is detected at a distance of 0 km off the coast, it is rare that the corresponding signal will be identified at a distance of 50 km. Thus, it is preferable to obtain satellite SST as close as possible to the shoreline in order to identify when coastal upwelling is occurring. However, it should also be noted, that the use of SST pixels that transgress the land/sea boundary is always bad practice, and often this approach is not encouraged (Tang et al., 2003). Additionally, our findings reveal that signal count within the OISST datasets, decreases with an increase in distance from the coastline. Conversely, the G1SST and CMC datasets displayed an increase in upwelling signals with an increase in distance from the shoreline. Furthermore, it was also evident that dissimilarities existed between products and sites when comparing the upwelling metrics. This may be due to the occasional satellite instrument outages such as result from satellite manoeuvres, or specifically with the MUR dataset, MUR pixels are identified as cloudy or fall in the inter-swath gap. The presence of clouds causes gaps in the data. Gaps between successive swaths of some sensors also lead to sampling errors. Sensors with narrower swaths are subject to a larger gap than others. MUR has unresolved SST variability on scales of 25 km in regions where extensive clouds are present, due to only microwave SSTs being used. Using microwave SSTs can reduce the sampling error caused by clouds, but there are sampling errors caused by precipitation. It is also possible that less upwelling signals are being detected close to the coastline in the CMC and G1SST dataset because of land heating thus increasing the SST and making upwelling not detectable (Ricciardulli et al., 2004).

It is important to note that the data sources are intrinsically different in the ways in which they were obtained or recorded. Consequently, one should not be too surprised to find large discrepancies; for example, the SACTN *in situ* collected SST product will reflect actual temperature of the water being measured, however instrumental differences exist; for example, whether the data were collected using a thermometer or an electric sensor. Satellite temperatures however, are collected remotely and sensors never have contact with the water. Here, bio-physical properties of IR and MW are related through complex algorithms to temperature (Minnett et al., 2002). Smit et al (2013) showed that warm and cold biases exist along the southern and western coastal region of South Africa, and the juncture between upwelling and non-upwelling regions have a tendency to influence on the variability and magnitude of the SST bias. When comparing SST products, a small bias does indeed exist, and is a result of solar flux, cloud cover as well as wind strength (Dufois et al. 2012). In conclusion the different data products, as used within this study, over the same geographical region, specifically the Benguela upwelling system have yielded different results. While flagging techniques are supposed to occasionally flag good values (Kilpatrick et al., 2001), it was found that flagging may occasionally be too vigorous for EBUS (Dufois et al., 2012). For example, the flagging method used on an OISST reference test induces warm coastal bias in data from both the MUR and G1SST data during summer. It should, however, be noted that this phenomenon can be explained by strong coastal SST gradients in these upwelling regions.

In the Benguela Upwelling system, as in many global regions, systematic, high resolution and wide coverage data sets of meteorological and oceanographic measurements are lacking. Global model outputs, reconstruction and reanalysis of datasets are potential solutions to this problem and thus provide data when none or only sparse information is available. Remotely sensed infrared SSTs have become a major data source and are instrumental in both oceanographic and atmospheric research (Dong et al., 2006). Despite the many factors that can influence how well the SST products reflect the climatological reality, these SSTs do show high degrees of correspondence with measurements obtained by buoys and other sources of *in situ* seawater temperatures measurements (Donlon et al., 2002; Smit et al., 2013). However, although SST products developed offshore and within the oceanic regions are being applied to the coastal regions, reports exist to inform users to exercise caution when using SST datasets in these coastal regions (Tittensor et al., 2010). Warm and cold biases have already been reported in several regions such as Australia (Blanchette et al., 2008), South Africa (Dufois et al., 2012) and China (Tang et al., 2003).

It must be kept in mind that variability does indeed exist, as described here in; the use of these products is dependent on their quality as well as homogeneity of the data. The spatial incompleteness and low accuracy problems associated with satellite SSTs limit product applications in oceanographic analyses, as well as air-sea temperature interaction studies. It is also evident that several physical processes such as inshore hydrodynamics operate in the mixed layer situated at the coastal region, and this may not be clearly detected by satellite temperature sensors. These processes include convection mixing due to cooling through evaporation, as well as tidal mixing and the injection of turbulence through breaking waves. Although progress in the analysis of sea surface temperature has been substantial in recent years, challenges do however remain. Improvements to the analyses are needed in areas where variability is substantial and sudden, namely near ocean fronts. Increased resolution and incorporation of *in situ* data would be among the avenues likely to yield a gain in accuracy within these areas (Brasnett, 2008). Studies often make use of broad scale phenomenon to define processes in the nearshore regions and vice versa; however, as illustrated within this study, events in the coastal region do not always coincide with or reflect those events of the offshore regions and vice versa.

Ample evidence suggests that satellite SST alone are not idea for coastal applications due to the presence of large biases. Contributing towards the magnitude of the biases are factors such as coastal proximity, presence of upwelling and coastal embayments. The coarser resolution of many existing SST products clearly has limitations in dynamic coastal regions, and the sampling capabilities in combination with the higher fidelity of moored buoys offer the potential for improving SST parameterizations in these regions. By excluding moored coastal buoys when merging multi-sensor SSTs, high- resolution analyses risk erroneously estimating the magnitude of the coastal SSTs; ultimately suppressing the high variability associated with small-scale processes in the coastal oceans. Data products representing upwelling signals with a duration exceeding 10 days may likely be related to an incorrect flagging of pixels affected by diurnal warming. Finally, concerns about satellite temperature accuracy changes in the ocean should make the accurate monitoring of seawater temperature a priority. Our results demonstrate that upwelling signals are more accurately detected at a distance of 0 and 25 km from the coastline and that MUR and G1SST data products have detected (albeit potentially erroneously) more upwelling signals lasting for longer durations.

CHAPTER 3

VARIATION OF UPWELLING SIGNALS DETECTED IN EBUS

Abstract

Global increases in temperature are severely altering land-sea temperature gradients. Bakun (1990) hypothesised that changes within these gradients will directly affect atmospheric pressure cells associated with the development of winds, and will consequently impact upwelling patterns within ecologically important Eastern Boundary Upwelling Systems (EBUS), which often act as 'buffers' that protect marine communities from the effects of ocean warming. In this study I used NOAA Optimally Interpolated sea surface temperature (SST) and ERA 5 reanalysis wind products to calculate an upwelling index which was used to detect, identify and quantify upwelling signals that have occurred throughout these EBUS over time last 37 years during summer months. Overall SST increased at three of the four EBUS currents, but there was a decrease in the number of signals detected and no significant increase in the intensity of these signals. The Humboldt current system in particular showed opposite trends with a decrease in SST and increase in the number of upwelling signals detected. Overall, these findings do not agree with the Bakun hypothesis.

Keywords: Climate change, Upwelling, Seawater temperature, coastal regions, Code: R

3.1. Introduction

Four major eastern boundary upwelling systems (EBUS) can be recognised (Bakun et al., 1991; Messié et al., 2009; Gruber et al., 2011; Pegliasco et al., 2015) each significantly impacting associated coastal systems. These systems are characterized as vast regions of coastal ocean occurring along the western shores of continents bordering the Pacific and Atlantic Oceans (Bakun, 1990; Pauly et al., 1995; Bakun et al., 2015, Bakun et al., 2010). The EBUS span a wide range of latitudes and are therefore spatially heterogeneous environments; the here referred to systems are the California (CCS), Humboldt (HCS), Canary (CnCS) and Benguela (BCS) current systems (**Figure 1**).

The complex interplay of biotic (biological) and abiotic (physical) processes, makes the EBUS of the world a popular focus for scientific research, as they are defined as high productivity regions covering <1% of the ocean area but provide up to 20% of the world's fishery output. The biological productivity in EBUS are mainly as a result of warm-season upwelling (Borges et al., 2003; Carr et al., 2003; Chavez et al., 2009; Rossi et al., 2009; García-Reyes et al., 2013). During the warm months, coastal winds strengthen by the development of land-based thermal low-pressure systems, often located east of oceanic high (OH) pressure systems (Huyer, 1983; Seager et al., 2003). Therefore, it is clear these regions provide both lucrative economic as well as significant recreational services to 10's of millions of people living along these coastlines. Recent studies have shown changes in the EBUS ecosystem structure (Fréon et al., 2009; Syndman, et al., 2014; Wang et al., 2015). Hence, monitoring changes across these systems are important.

Recognising that the cross-shore atmospheric pressure gradients lead to alongshore, equatorward winds that drive coastal upwelling, Bakun (1990) hypothesized that an increase in upwelling favourable winds due to intensification o the continental oceanic pressure gradient under climate change, with several other studies showing that upwelling favourable winds intensify (Bakun, 1990; Sydeman et al 2014; Garca-Reyes et al., 2015). Both the past and current records are currently still debated, with conflicting results being reported. Research done by Narayan et al., (2010) shows decreasing trends in California; Dewitte et al., (2012) and Tim et al., (2015) reported no signficant trends in the BCS and HCS. Pardo et al., (2011) showed decreasing upwelling in the CnCS. This lack of agreement and coastal warming makes any assessment of future coastal processes challenging. Coastal warming increases the water stratification which ultimately limits the effectiveness of upwelling. An increase and decrease in upwelling favourable winds can also amplify or reduce the effect of coastal warming. Therefore, changes in upwelling favourable winds are important.

Many of the significant upwelling modifications in EBUS, particularly in the Pacific Ocean, has been attributed to large scale atmospheric processes (Jacox et al., 2015). ENSO is the leading cause of variability in the HCS and CCS (Minobe et al., 1999). Other factors such as the Pacific Decadal Oscillation (PDO), and the North Pacific Gyre Oscillation (NPGO) are also liked to the variability CCS (Chhak et al., 2007; DiLorenzo et al., 2008). The BCS however appears to not be affected by the basin-scale thermocline but rather it is highly influenced by small scale variability (Chavex et al., 2009). Several studies contribute to researching EBUS, however there are no studies that report shared variability across all EBUS. In this context, with the predictions that climate change ultimately leads to a more intense upwelling signal, the focus of this study is to assess the variation in the intensity and duration of upwelling signals overtime by using OISST data and ERA 5 wind products.

3.2. Methods

3.2.1. Data

We are specifically interested in observing variations in upwelling signals detected over a period of time. To evaluate if there are changes in duration, frequency and intensity, this study made use of the gridded data of the global 0.25° AVHRR-only O12 Optimally-Interpolated Sea Surface Temperature (OISST). This data is constructed by combining different data collected from satellites, ships and buoys (Reynolds et al., 2007; Banzon et al., 2016). OISST provides global fields that are based on a combination of ocean temperature observations and in situ platforms. This data has been collected for more than four decades hence providing us with a long enough time series from which upwelling metrics and their rate of change can be calculated.

In order to detect variation in upwelling signals and wind patterns among the four EBUS (**Figure 3.1)** (Bakun, 1990; Bakun et al., 2015), wind speed and direction were deemed as important variables along with temperature. Wind speed and direction variables were downloaded from the ERA5 climate reanalysis produced by ECMWF, providing hourly data on regular latitude-longitude grids at 0.25° x 0.25° resolution. This dataset was used to compute the upwelling index which was used to identify when upwelling signals were present. Average intensity of signals was then calculated as the slope of the linear regression versus time.

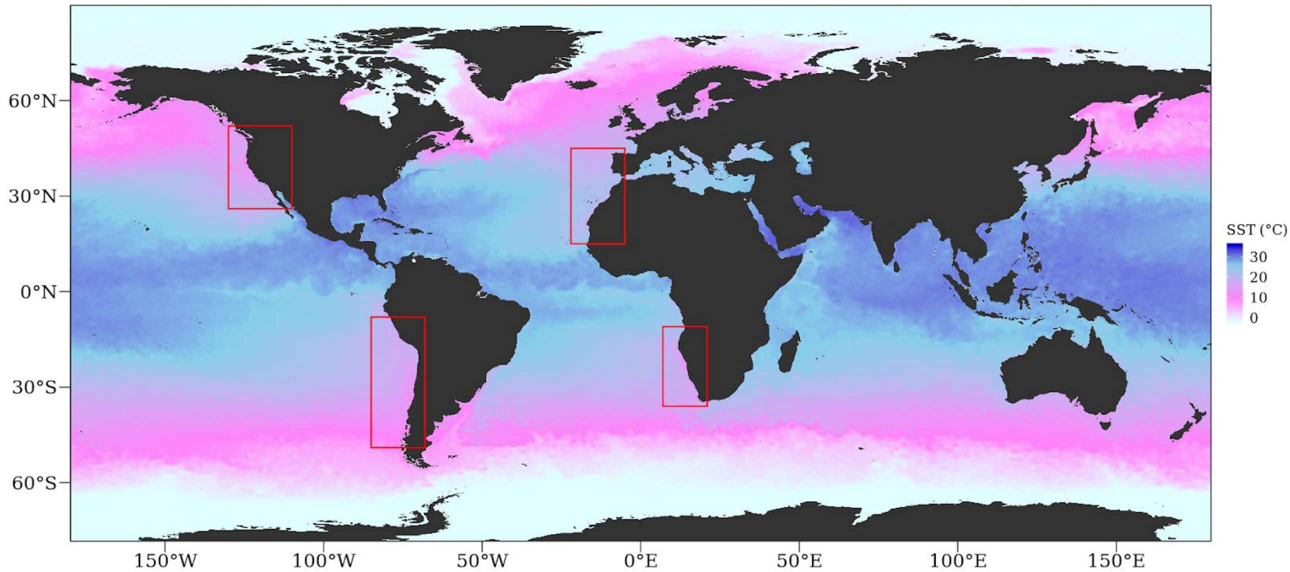

Figure 3.1: OISST throughout the global ocean. The red coloured squares delimit EBUS: California (CCS), Humboldt (HCS), Canary (CnCS) and Benguela (BCS) current systems.

3.2.2. Upwelling identification

In order to determine whether changes exist in the frequency and duration of upwelling signals across EBUS it is important to first identify when upwelling was occurring; however, in order to do this a set of upwelling threshold values needed to be established when the phenomenon was occurring; because upwelling is affected by wind, both wind and SST data were used. This unique method of determining upwelling signals considers both SST and wind variables which narrows these signals down to a more definite scale. The wind data was used in order to calculate the upwelling index using the formula presented in Fielding et al., (1989). The index relies heavily on wind speed and wind direction data in order to determine the presence of upwelling. Where an upwelling index value of less than 0 represented down-welling, and greater than 0 represented upwelling Fielding et al., (1989). When the upwelling index was greater than 0 the SST drops, as expected, thus suggesting that upwelling is occurring. This drop in SST that coincided with a positive upwelling index value was close to the seasonal variation of 25th percentile threshold for SST. Thus, the SST and upwelling index value was used to determine when an upwelling phenomenon was occurring. It was then necessary to determine the number of consecutive days that must be exceeded for an upwelling signal to be identified as a discrete event. Here it must be noted that upwelling is known to vary on a seasonal basis and may also occur hourly (sub-daily). Therefore, the minimum duration for the classification of an upwelling signal was set as one day. The rationale behind this was that the OISST dataset is collected at a daily resolution. With the upwelling index, temperature and duration thresholds established, the `detect_event()` function from the ***heatwaveR*** package (Schlegel et al., 2018) was used to calculate metrics for the upwelling signals. By using this method of identifying signals, we are able to gain metrics such as the intensity and duration, which allows us to compare variation in these metrics over time. Because upwelling signals were calculated relative to percentile exceedances, rather than an absolute definition such as temperatures below a fixed temperature threshold, these signals could occur any time of the year, however, upwelling was shown to be more dominant during spring and summer months, as expected.

3.3. Results

Overall, it was found that of the four investigated EBUS currents, the CnCS had the highest upwelling intensity. In addition, three of the four currents showed increases in mean upwelling intensity, while the CCS current showed a decrease in intensity (**Table 3.1**). In terms of the cumulative intensity of upwelling signals, the BCS current had the greatest increase over time when compared to its three contemporaries. Moreover, when comparing upwelling signal metrics across EBUS currents using a series of general linear hypotheses it was found that significant differences in the duration of upwelling signals were present between currents during the summer seasons ($F = 3.608$, SS = 9210, $p < 0.05$). However, there were no significant difference in the mean intensity of currents ($F = 0.26$, SS = 119, $p < 0.98$), the cumulative intensity ($F = 0.81$, SS = 2257, $p = 0.88$) of currents, nor the maximum intensity ($F = 0.24$, SS = 99.8, $p = 0.86$) of signals detected during these months.

Table 3.1: Mean and cumulative intensity values for upwelling signals in EBUS during summer months; the EBUS column displays the four EBUS currents that form the focus of this study. The mean intensity is defined as the mean temperature anomaly value during the upwelling signal; the Cumulative intensity Colum is the sum of the daily intensity anomalies over the duration of the upwelling signal.

EBUS	Mean intensity (°C)	Cumulative intensity (°C.days)
BCS	0.86	3.24
CCS	-9.47	-14.48
CnCS	4.25	-33.56
HCS	0.79	2.52

My investigations of the trends within individual time series data for each of the four EBUS currents revealed variables patterns of SST changes have occurred within each site over the past 37 years (**Figure 3.2**). I found that the BCS displayed a slow positive increase in SST of approximately 0.17 ± 0.02 °C/decade, and increases here were particularly prominent during January of each year. Similarly, the CCS also showed an increase in SST with a positive trend of 0.20 ± 0.02 °C/decade, with it's steepest increases occurring during June. The CnCS continually shows warming trends of 0.20 ± 0.01 °C/decade, with August representing the steepest increase of 0.20 °C/decade. Overall, the SST of the BCS and CnCS currents increased by approximately 0.21 °C over a period of 37 years. These results correspond to the findings of Seabra et al. (2019), which demonstrate warming rates of approximately 0.06 °C/decade. Conversely, the HCS expressed a negative linear trend demonstrating a decrease in SST over this same time period, suggesting that the HCS can be classified as the only EBUS with a consistent negative SST trend.

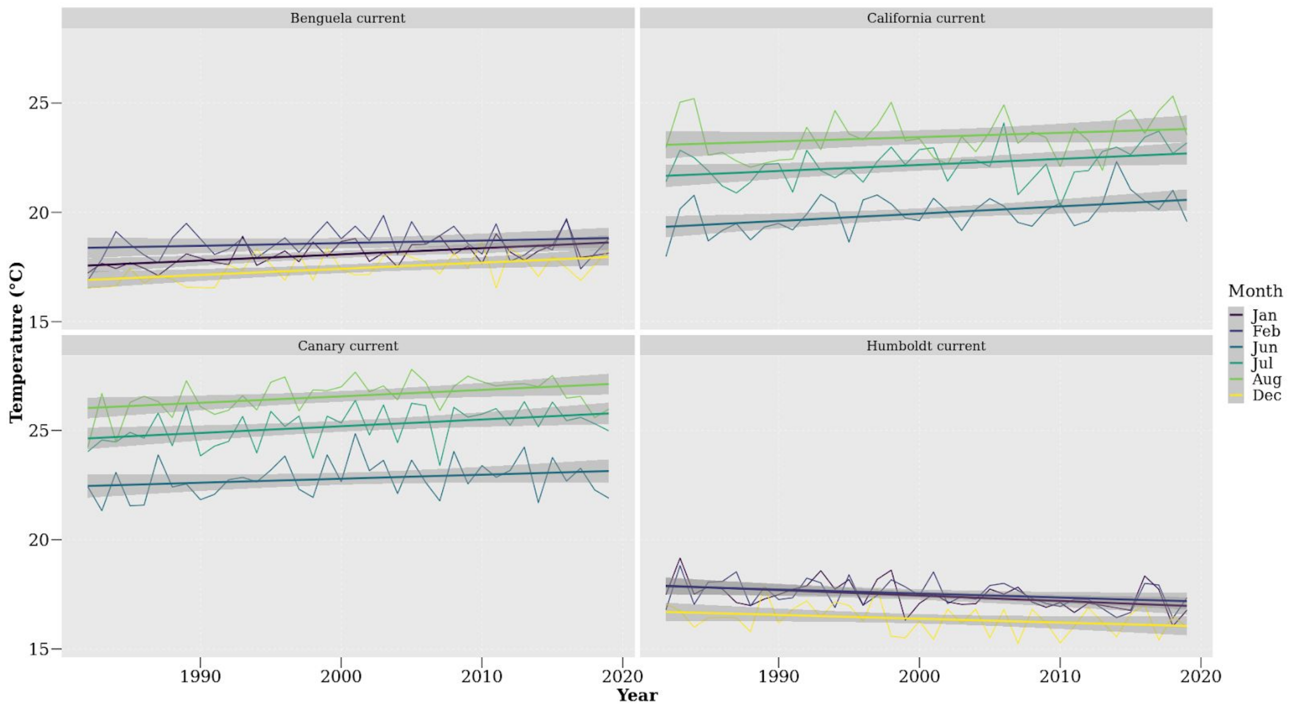

Figure 3.2: SST summer trends in the northern and southern hemisphere over a period of 37 years.

Regarding trends of wind intensity at each of the four EBUS currents during summer months, I found that overall minor increases have occurred at each EBUS over the past 37 years. Within the BCS, wind intensity increased by 0.02 ± 0.0 m.s^{-1}/decade during the months of January and February but decreased by 0.002 m.s^{-1}/decade during December. In the CCS, wind intensity increased by 0.01 m.s^{-1}/decade during July and August that was preceded by a negative trend over the month of June, of 0.02 m.s^{-1}/decade. The CnCS had a slightly positive trend in wind intensity for the summer months ranging between 0.07 ± 0.04 m. s^{-1}/decade. The wind intensity in the HCS shows a more negative trend during January and February, of 0.06 ± 0.01 m. s^{-1}/decade followed by an increase of 0.08 m. s^{-1}/decade in December.

Results of a two-way ANOVA test revealed that a significant difference exists between wind intensity for each of the currents (F = 472.19, SS = 151.18, p < 0.002), along with no significant distinction in wind speed spanning each year among the currents (F = 0.97, SS = 0.31, p = 0.40). Because wind intensity represented no significant difference over time, I also chose to observe if changes exist in the duration of wind blowing in a south-easterly direction. These subsequent findings indicated that a significant difference in the duration of south-easterly wind exists between the four currents (F = 2547.46, SS = 22266, p < 0.002). The HCS represented the site with the longest duration of south easterly winds as compared to the remaining three EBUS currents. However, there was no significant difference in the duration of winds over time (F = 0.706, SS = 2, p = 0.40). Moreover, when comparing monthly changes in wind intensity within each EBUS region I found that the BCS and CnCS respectively showcased negative trends (BCS: R^2 =0.006 ± 0.04, CnCS: R^2 = 0.003 ± 0.02), whereas the CCS and HCS respectively showcased overall positive trends (CCS: R^2 0.08 ± 0.16, HCS: R^2 = 0.003 ± 0.04).

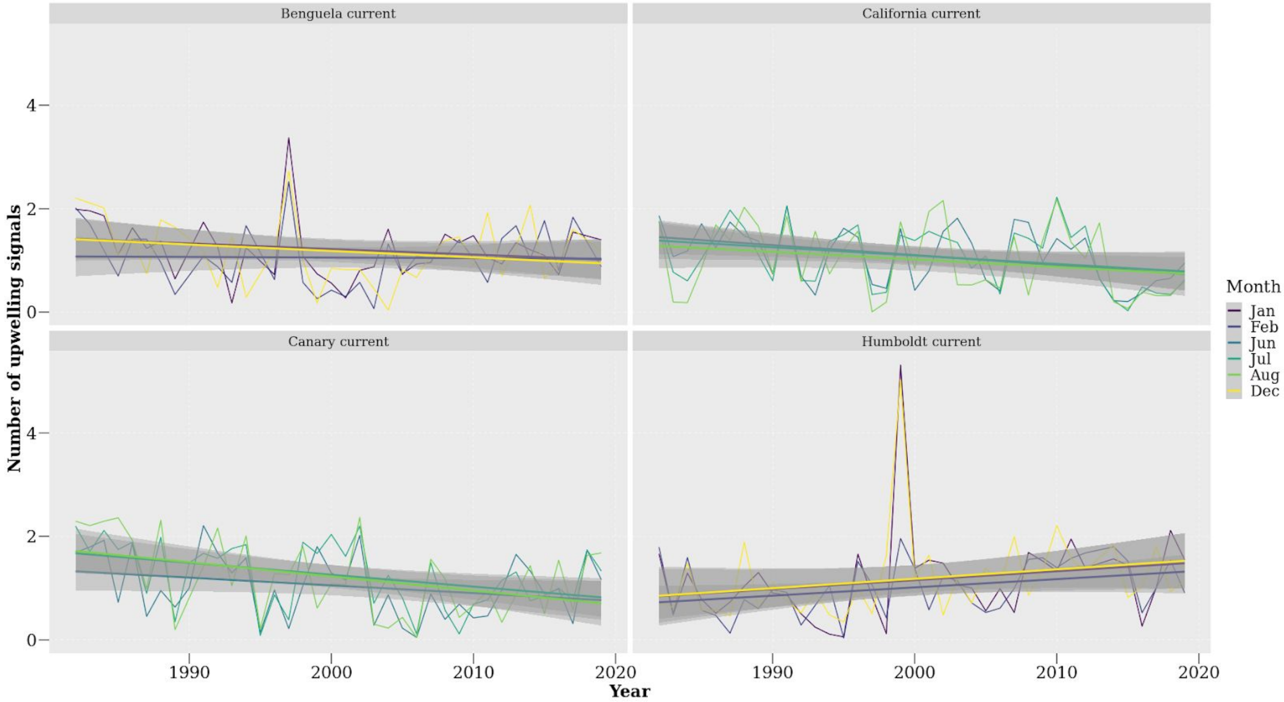

Figure 3.3: Number of upwelling signals detected in the summer months of the northern and southern hemisphere over a period of 37 years.

Lastly, I found that the number of upwelling signals detected decreased over time during summer months in the BCS, CCS and the CnCS, and slightly increased within the HCS current (**Figure 3.3**). This increase is particularly dominant during December, contrasting with decreasing SST temperature values Results obtained from a two-way ANOVA revealed a significant difference in the number of signals detected each year (F = 7.70, SS = 3.03, p = 0.005) and between currents (F = 10.19, SS = 12.01, p < 0.001).

3.4. Discussion

Bakun (1990) proposed that an increase in greenhouse gases will result in considerable change towards land-sea pressure gradients that will affect global wind patterns and ultimately result in an increase in the intensity of upwelling signals across the world's oceans. Here, I tested this hypothesis by analysing upwelling trends at four prominent upwelling regions, and with an emphasis on summer as this is when upwelling is most dominant. Our results yielded insignificant evidence for increases in the intensity of upwelling signals at each of the four major EBUS currents across the southern and northern hemispheres of the world's oceans., However, I have found evidence that suggests there is a significant difference in the duration of upwelling signals detected over time across these four regions. Given that the intensity of upwelling did not intensify at these sites, I further investigated if SST and wind patterns have changed there over time. When observing the SST patterns within EBUS currents it was evident that the average temperature across all EBUS currents are continually increasing, except at the HCS. However, the same was not true of wind intensity as I found no significant relationship between increased wind intensity and time at the different EBUS regions. Instead I found that there was a significant difference between currents with respect to the number of days (duration) that the wind blew in a south-easterly direction. By combining wind and SST products I was able to observe trends in the number of upwelling signals detected. Our results suggested a decrease in three of the EBUS besides the HCS which showed an increase in the number of upwelling signals detected over a period of 37 years.

The sensitivity of upwelling intensity was consistent with more focused analyses of the HCS (Belmandani et al., 2014). Belmandani et al., (2014) describes the intensity of upwelling to changes in the location and intensity of the oceanic high-pressure system, and demonstrates the need to consider both geostrophic and ageostrophic processes affecting the boundary layer of the coastal ocean. These analyses may offer more information regarding the dynamics at play in regulating changes in other upwelling zones. However, it should be noted that Rykaczewski et al. (2015) also suggested that an increase in land-sea pressure gradient (which drives wind patterns) has not stimulated an increase in upwelling over the past decades.

Given my findings here, it is evident that the effects of anthropogenic changes towards altering patterns of upwelling are more complex than proposed by Bakun (1990) and demonstrates the need to consider changes in both thermal and hydrodynamic (i.e. water vapour content) processes when interpreting the full dynamical response of the coupled atmospheric-ocean system to climate warming. In this regard, our conclusion differs in respect to recent studies (for example, Wang et al., 2015) that have examined the relationship between increasing summertime land-sea temperature differences and intensified upwelling in response to climate change. For example, Rykaczewski et al., (2015) suggested that increased land-sea temperature differences are ubiquitous into projections of future conditions, but that summertime upwelling is limited to the polar extremes of upwelling zones. If true, this would indicate that increased land-sea temperature differences do not have a dominant influence on upwelling intensity. Additionally, changes in upwelling favourable winds are not always directly related to broad increases in land-sea temperature differences associated with climate change. Instead, the intensity of upwelling-favourable winds could be related to shifts in seasonal development and geographic positioning of the four major atmospheric high-pressure systems that are completely unrelated to anthropogenic influences. Research suggest (Gillett et al., 2013; Griffies et al., 2014) that changes in sea level pressure (SLP) fields are expected in response to increased greenhouse gas concentration; these shifts will initiate changes in the magnitude, location and timing of upwelling favourable winds that are more consequential than increase land-sea temperature differences.

The results obtained in this study does not support the hypothesis that intensified upwelling will result from the increased land-sea difference associated with global warming. Additionally, given the short time series it is highly likely that a natural climatic variable impacted the trends discussed. For example, the occurrence of ENSO at the end of the time series could also have initiated an anomalously warm SST in EBUS and potentially affect the trends observed. Further investigation is required to fully explain the observed trends in upwelling within EBUS regions. Such investigations should ideally directly focus on the impact of inter-annual variability within individual EBUS currents. My results also lead to speculation about the potential connection between ENSO in the CCS (Peterson et al., 2003; Blamey et al., 2012; Sydeman et al., 2013). ENSO represents a weakening of the walker cell circulation. During normal walker cell conditions there is consistent upwelling, this upwelling contributes to cool SST. Since the data in CnCS shows an increase in SST, it may also be concluded that there has been a weakening or reversal of the trade winds and a resultant El Nino is occurring. ENSO is another climatic variable which are able to increase SST. ENSO sends out atmospheric and oceanic Rossby waves that can have an effect on climate processes. The effects ENSO has on its counterpart La Nina produces teleconnection that alter average climatic states. As a result, it can also be assumed that the weakening of HCS is potentially represented as a consequence of the effects by La Nina. During La Nina, the walker cell circulation is enhanced, meaning that pre-existing trade winds and SST strengthen. The low SSTs created by the presence of La Nina is accompanied by anticyclones. The anticyclones rotate counter-clockwise in the southern hemisphere and therefore its winds travel equatorward where they deflect surface water away from the shore, resulting in a net ekman spiral that encourages coastal upwelling and lowers SSTs. The HCS possessed the strongest winds when compared to the other EBUS. These winds are comprised of dry air creating climatic conditions that encourage evaporation. Evaporation requires heat, and this heat is supplied by the sea surface. Since evaporation takes heat away from the sea surface it has an overall cooling effect. For the CnCS, the enhanced evaporation caused by the strong offshore winds result in a cooling of the current system's SSTs. The CnCS are defined as a high-pressure system which are typically characterized by generating a climate with low cloud coverage. Low cloud coverage allows for a high amount of solar radiation to be received at the surface.

There is low confidence regarding the effects of climate change on coastal temperatures and biogeochemistry in the EBUS. However, consideration is now given to shifts in the intensity and latitudinal location of upwelling, and will be essential for identifying portions of the coast more at risk of ocean acidification, increased hypoxia, and eutrophication under conditions of future warming (Rykaczewski et al., 2015). This is primarily due to the complex global and local processes affecting these patterns, but also largely due to the resolution and data availability combined with the large degree of decadal variability in temperatures and biogeochemical properties. Most of the remotely sensed SST and wind products do not have sufficient resolutions to accurately detect nuances within the upwelling process. Nevertheless, these data sources show promise in correcting bias by including higher-resolution products which consider land-and ocean-air interactions, cloud formation, and oceanic mesoscale processes. Furthermore, changes in local, alongshore winds are among one of several processes necessary to consider when exploring the sensitivity of upwelling in relation to climate change (Bakun et al., 2015).

Waters supplied to upwelling systems, including nutrient concentrations, as well as the characteristics of the ocean carbonate system, and dissolved oxygen levels are sensitive to climate change (Rykaczewski et al., 2010) and have important ecological impacts (Lu et al., 2010). Additionally, changes in water-column stratification can alter upwelling efficacy (Roemmich et al., 1995; Chhak et al., 2007), and the offshore distribution of maximal upwelling (in addition to associated changes in wind-stress curl) can influence the rate and spatial location of upwelling (Rykaczewski et al., 2008; Jacox et al., 2014). Interactions among basin-scale processes and subsurface biogeochemistry that alter source-water properties of upwelled water masses, stratification, and mesoscale hydrographic features should be considered in concert with atmospheric forcing to develop a comprehensive understanding of the implications of climate change for the world's upwelling ecosystems. However, given the natural variability of EBUS, they are proven to be more resilient to climate change when compared to other ecosystems. The lack of expectations for EBUS ecosystems is of concern because these regions are biologically rich and as a result are highly relevant to society with regards to economics, conservation and biodiversity.

CHAPTER 4

SYNTHESIS AND CONCLUSIONS

4.1. Upwelling in various SST products

In the first study of this thesis, I sought to make use of the SACTN *in situ* collected data and satellite SST products to identify and compare upwelling signals between the various SST products and at various distances from the coastline by using a novel method of identifying upwelling signals. This study is important in demonstrating the differences between SST products and their varied resolutions. Here upwelling signals are used as a known signal in the data and allows for a comparison between data products allowing us to observe the importance of the resolutions of data products.

4.2. Upwelling in the EBUS

After demonstrating the capacity to identify upwelling signals using a novel method in the first study, the second study aimed to focus on quantifying trends relating to upwelling signals within ecologically important EBUS currents over the past 37 years. Bakun (1990) proposed that an increase in climate change resulting from increased quantities of greenhouse gasses may fundamentally alter pressure gradients that will affect wind patterns and ultimately increase upwelling over prolonged periods. In this study, I disproved Bakun's hypothesis using my novel method that considers both SST and wind variables. Importantly, this method differs from previous methods to determine upwelling and currently represents the most effective means for identifying metrics of upwelling.

4.3. Contributions

SST datasets are often products resulting from blends of both *in situ* and satellite analyses. The *in situ* collected data is used to provide a benchmark for temperature recordings, and the satellite analyses is used to define the shape of the final product between the benchmarks. It is proven that blended techniques are an effective way to improve satellite coverage with eliminating a large portion of the bias that exists between the *in situ* and satellite data. Adjustments to correct for in-homogeneities in SSTs in recent years have a large impact on the resulting decadal-scale of global temperature trends. Changes to weather station equipment have only had a modest effect over the past two centuries but can be corrected for by using the metadata and interstation comparison (Menne et al., 2009; Hausfather et al., 2016). By contrast, SST products have been measured using floating buoys, insulated buckets, ship sensors, with each of these different systems measuring at different depths (Cowtan et al., 2018). Various methods are used to homogenize sea surface temperature observations, be it the use of metadata in order to determine the method used for a given observation, along with field replication, and reconciliation of different observation types to correct for the heterogeneous observation systems (Parker et al., 1995; Rayner et al., 2006; Kennedy et al., 2011). Another approach to homogenise SST is by making use of night time marine air temperature observation as a reference against which to correct the SST observations from ships. Given the various techniques and data resolution, different data products at different resolutions are predicted to show slight variation in their data.

As seen in chapter 2, the higher resolution data, the G1SST data products detected the highest number of upwelling signals. The signals detected often lasted for longer when compared to the OISST, CMC and SACTN data products. However, even though they detected signals with the longest duration, most of the signals detected lasted for a period of approximately 10 days as seen in the OISST, CMC and SACTN data products. The results also showed that upwelling varies at different distances from the coastline and that the higher resolution data would more likely detect upwelling at a further distance from the coastline compared to the lower resolution data. As such, while higher resolution data produced overall superior detections, the limitations of the data products of broader resolutions did not severely alter the results but the effects were noticeable.

SST datasets are often products resulting from blends of both in situ and satellite analyses. The in situ collected data is used to provide a benchmark for temperature recordings, and the satellite analyses is used to define the shape of the final product between the benchmarks. It is proven that blended techniques are an effective way to improve satellite coverage with eliminating a large portion of the bias that exists between the in situ and satellite data. Adjustments to correct for in-homogeneities in SSTs in recent years have a large impact on the resulting decadal-scale of global temperature trends. Changes to weather station equipment have only had a modest effect over the past two centuries but can be corrected for by using the metadata and interstation comparison (Menne et al., 2009; Hausfather et al., 2016). By contrast, SST products have been measured using floating buoys, insulated buckets, ship sensors, with each of these different systems measuring at different depths (Cowtan et al., 2018). Various methods are used to homogenize sea surface temperature observations, be it the use of metadata in order to determine the method used for a given observation, along with field replication, and reconciliation of different observation types to correct for the heterogeneous observation systems (Parker et al., 1995; Kennedy et al., 2011). Another approach to homogenise SST is by making use of night time marine air temperature observation as a reference against which to correct the SST observations from ships. Given the various techniques and data resolution, different data products at different resolutions are predicted to show slight variation in their data.

As seen in chapter 2, the higher resolution data, the G1SST data products detected the highest number of upwelling signals. The signals detected often lasted for longer when compared to the OISST, CMC and SACTN data products. However, even though they detected signals with the longest duration, most of the signals detected lasted for a period of approximately 10 days as seen in the OISST, CMC and SACTN data products. The results also showed that upwelling varies at different distances from the coastline and that the higher resolution data would more likely detect upwelling at a further distance from the coastline compared to the lower resolution data. As such, while higher resolution data produced overall superior detections, the limitations of the data products of broader resolutions did not severely alter the results but the effects were noticeable.

The homogenization of the sea surface temperature record is challenging, and this is often as a result of changing observation platforms and variability in the observation protocol. Metadata and combination of external temperature sources have been used to homogenize the data products used within this thesis, with differing results. This uncertainty is known to arise from under-sampling of variability and the uncertainty in the estimated bias corrections (Rayner et al., 2005). It is also noted that different countries provide different advice to their observing fleets concerning how best to measure SST. Additionally, modern SST buckets are prone to heat loss, especially when air and sea temperatures differences are large (Kent et al., 2006). Similarly, engine intake SST has displayed a biased warm trend in the past but has shown a cold bias since the 1990s. Specifically, the MUR data ingests 1-km resolution of MODIS SST, the MUR data also improves the analysed feature resolution y an order of magnitude over most of the existing SST analyses products from approximately 100 km down to 10 km. The MUR data also agrees with the 0.25° ×0.25°-gridded GMPE median SST analysis to 0.36°C on average, where differences among the existing SST analyses are large (Castro et al., 2016). The MUR data product makes use of a MRVA interpolation method (Chin et al., 2014), this method avoids truncation of the geolocation information and preserves intra-grid features. However, differences are large between the data products that make up the MUR dataset and this affects the accuracy of the SST. The other SST products contributing to the MUR SST data product such as the MODIS SST has shown to incorporate a small bias, this is expected due to solar heating in the morning and afternoon. This bias is dependent on solar flux and wind strength (Gentemann et al., 2003). However, while SST flagging techniques are supposed to occasionally flag good values (Kilpatrick et al., 2001), it was found that flagging may be too vigorous and too systematic in upwelling regions, and SST values in some regions are not representative during summer and peak upwelling seasons (Dufois et al., 2012).

A flagging method based on the OISST data induces a warm bias during summer. This is explained by the strong SST gradient in the coastal region that cannot be accurately represented by the large scale OISST product. The warm bias however does not however present the same extent in all EBUS, but also a decrease of this bias is also different in the various systems (Dufois et al., 2012). For example, the southern Benguela, which exhibits the strongest warm bias, presents the strongest zonal SST gradients. On the contrary, in the California system, which presents the weakest climatological zonal SST gradients, the bias is almost completely removed in the new Pathfinder data (Dufois et al., 2012). The presence of aerosols affected satellite SST retrievals as data products often cannot make retrievals during cloud-covered regions which are extremely dominant in the Southern Ocean (Dong et al., 2006). Research by Ricciardulli et al., (2004) suggests that both infrared and microwave observation of the ocean temperature can benefit from their comparison. For example, the comparison of SSTs obtained from a number of IR algorithms with other independent SST observations (TMI, Reynolds OI or buoys) can help identify the optimal IR algorithm in terms of accuracy.

When observing patterns in upwelling signals over a period of 37 years it is evident that the effects of anthropogenic changes towards altering upwelling intensity is more complex than proposed in the Bakun hypothesis (1990). When determining upwelling, both thermal and hydrodynamic processes should be considered. This research study does not support the hypothesis that intensified upwelling will result because of global warming. However, given the short time series and limited variables used in this study, the results could have been influenced by other natural climatic variables, which impacted the results.

4.4. Further research

By using the detect_event() function in the heatwaveR package which provide several metrics used in order to quantify the events or upwelling signals such as cumulative intensity is of high importance as this is regarded as the most relevant information in ecologically, as it is used to quantify the risk that and even or upwelling signal may have on the ecosystem. This would then allow one to determine the impact changes in these systems will have on its surrounding ecosystems. Ultimately this would be of high importance for conservation, as well as studies into social and economic security associated with upwelling. Understanding upwelling, its changes and it's the effect on coastal systems will prove necessary if coastal ecosystems are to truly be conserved.

More work should be done on the improvement of the methodology to understand and include both atmospheric and oceanographic states during upwelling. Specifically, it is of our interest to share the code developed and used within this thesis in order to allow for improvement in usability and reproducibility of this research. Once all of these variables are quantified and inducted into its calculations, this knowledge should then be paired with forecast products to see how effective and accurate this research is and to forecast upwelling signals and the impact it has on the associated ecosystems. The main goal of this thesis was not to predict events or signals but rather to use this novel method of determining upwelling signals and to use this method to conduct an investigation that observe trends in upwelling patterns over time given the Bakun hypothesis and to observe if the same upwelling signals persist in data of various resolutions and distances from the coastline. Ultimately it is hoped that forecasting upwelling signals and the adoption of subsequent future policies to better prepare for these phenomena will result in a positive economic impact.

REFERENCES

Aguirre, C., Rojas, M., Garreaud, R.D. and Rahn, D.A., 2019. Role of synoptic activity on projected changes in upwelling-favourable winds at the ocean's eastern boundaries. *npj Climate and Atmospheric Science*, *2*(1), pp.1-7.

Alves, J.M. and Miranda, P.M., 2013. Variability of Iberian upwelling implied by ERA-40 and ERA-Interim reanalyses. *Tellus A: Dynamic Meteorology and Oceanography*, *65*(1), p.19245.

Arístegui, J., Barton, E.D., Álvarez-Salgado, X.A., Santos, A.M.P., Figueiras, F.G., Kifani, S., Hernández-León, S., Mason, E., Machú, E. and Demarcq, H., 2009. Sub-regional ecosystem variability in the Canary Current upwelling. *Progress in Oceanography*, *83*(1-4), pp.33-48.

Arntz, W.E., Gallardo, V.A., Gutiérrez, D., Isla, E., Levin, L.A., Mendo, J., Neira, C., Rowe, G.T., Tarazona, J. and Wolff, M., 2006. El Niño and similar perturbation effects on the benthos of the Humboldt, California, and Benguela Current upwelling ecosystems.

Bakun, A., 1990. Global climate change and intensification of coastal ocean upwelling. *Science*, *247*(4939), pp.198-201.

Bakun, A. and Nelson, C.S., 1991. The seasonal cycle of wind-stress curl in subtropical eastern boundary current regions. *Journal of Physical Oceanography*, *21*(12), pp.1815-1834.

Bakun, A., 1996. Patterns in the ocean: ocean processes and marine population dynamics, 323 pp. *University of California Sea Grant, San Diego & Centro de Investigaciones Biológicas del Noroeste, La Paz*.

Bakun, A. and Weeks, S.J., 2004. Greenhouse gas buildup, sardines, submarine eruptions and the possibility of abrupt degradation of intense marine upwelling ecosystems. *Ecology Letters*, *7*(11), pp.1015-1023.

Bakun, A., Field, D. B., Redondo‐Rodriguez, A.N.A. and Weeks, S .J. (2010). Greenhouse gas, upwelling‐favorable winds, and the future of coastal ocean upwelling ecosystems. *Global Change Biology*, *16*(4), pp.1213-1228.

Bakun, A., Black, B.A., Bograd, S.J., Garcia-Reyes, M., Miller, A.J., Rykaczewski, R.R. and Sydeman, W.J., 2015. Anticipated effects of climate change on coastal upwelling ecosystems. *Current Climate Change Reports*, *1*(2), pp.85-93.

Barange, M., Gibbons, M.J. and Carola, M., 1991. Diet and feeding of Euphausia hanseni and Nematoscelis megalops (Euphausiacea) in the northern Benguela Current: ecological significance of vertical space partitioning. *Marine Ecology Progress Series*, pp.173-181.

Barton, E.D., Field, D.B. and Roy, C., 2013. Canary current upwelling: More or less?. *Progress in Oceanography*, *116*, pp.167-178.

Barton, C.A., McCormack, J.P., Eckermann, S.D. and Hoppel, K.W., 2019. Optimization of Gravity Wave Source Parameters for Improved Seasonal Prediction of the Quasi-Biennial Oscillation. *Journal of the Atmospheric Sciences*, *76*(9), pp.2941-2962.

Baumann, H. and Doherty, O., 2013. Decadal changes in the world's coastal latitudinal temperature gradients. *PloS one*, *8*(6), p.e67596

Beaufort, L., de Garidel-Thoron, T., Mix, A.C. and Pisias, N.G., 2001. ENSO-like forcing on oceanic primary production during the late Pleistocene. *Science*, *293*(5539), pp.2440-2444.

Belkin, I.M., 2009. Rapid warming of large marine ecosystems. *Progress in Oceanography*, *81*(1-4), pp.207-213.

Bjerknes, J., 1969. Atmospheric teleconnections from the equatorial Pacific. *Mon. Wea. Rev*, *97*(3), pp.163-172.

Blanco, J.L., Thomas, A.C., Carr, M.E. and Strub, P.T., 2001. Seasonal climatology of hydrographic conditions in the upwelling region off northern Chile. *Journal of Geophysical Research: Oceans*, *106*(C6), pp.11451-11467.

Blanchette, M.L. and Pearson, R.G., 2012. Macroinvertebrate assemblages in rivers of the Australian dry tropics are highly variable. *Freshwater Science*, *31*(3), pp.865-881.

Blamey, L.K., Howard, J.A., Agenbag, J. and Jarre, A., 2012. Regime-shifts in the southern Benguela shelf and inshore region. *Progress in Oceanography*, *106*, pp.80-95.

Bograd, S.J., Schroeder, I., Sarkar, N., Qiu, X., Sydeman, W.J. and Schwing, F.B., 2009. Phenology of coastal upwelling in the California Current. *Geophysical Research Letters*, *36*(1).

Borges, M.F., Santos, A.M.P., Crato, N., Mendes, H. and Mota, B., 2003. Sardine regime shifts off Portugal: a time series analysis of catches and wind conditions. *Scientia Marina*, *67*(S1), pp.235-244.

Boyd, A.J., Salat, J. and Masó, M., 1987. The seasonal intrusion of relatively saline water on the shelf off northern and central Namibia. *South African Journal of Marine Science*, *5*(1), pp.107-120.

Boyer, D.C. and Hampton, I., 2001. An overview of the living marine resources of Namibia. *African Journal of Marine Science*, *23*, pp.5-35.

Brasnett, B. (200)8. The impact of satellite retrievals in a global sea‐surface‐temperature analysis. *Quarterly Journal of the Royal Meteorological Society*, *134*(636), pp.1745-1760.

Brady, R.X., Alexander, M.A., Lovenduski, N.S. and Rykaczewski, R.R., 2017. Emergent anthropogenic trends in California Current upwelling. *Geophysical Research Letters*, *44*(10), pp.5044-5052.

Brown, O. B., Brown, J. W. and Evans, R. H. (1985). Calibration of advanced very high resolution radiometer infrared observations. *Journal of Geophysical Research: Oceans*, *90*(C6), pp.11667-11677.

Bulgin, C.E., Embury, O. and Merchant, C. J. (2016). Sampling uncertainty in gridded sea surface temperature products and Advanced Very High Resolution Radiometer (AVHRR) Global Area Coverage (GAC) data. *Remote Sensing of Environment*, *177*, pp.287-294.

Capet, X.J., Marchesiello, P. and McWilliams, J.C., 2004. Upwelling response to coastal wind profiles. *Geophysical Research Letters*, *31*(13).

Cardone, Vincent J., Juliet G. Greenwood, and Mark A. Cane. "On trends in historical marine wind data." *Journal of Climate* 3, no. 1 (1990): 113-127.

Carr, M.E., 2001. Estimation of potential productivity in Eastern Boundary Currents using remote sensing. *Deep Sea Research Part II: Topical Studies in Oceanography*, *49*(1-3), pp.59-80.

Carr, M.E. and Kearns, E.J., 2003. Production regimes in four Eastern Boundary Current systems. *Deep Sea Research Part II: Topical Studies in Oceanography*, *50*(22-26), pp.3199-3221.

Casabella, N., Lorenzo, M.N. and Taboada, J.J., 2014. Trends of the Galician upwelling in the context of climate change. *Journal of sea research*, *93*, pp.23-27.

Chao, Y., Li, Z., Farrara, J. D. and Hung, P. (2009). Blending sea surface temperatures from multiple satellites and in situ observations for coastal oceans. *Journal of atmospheric and oceanic technology*, *26*(7), pp.1415-1426.

Chaigneau, A., Eldin, G. and Dewitte, B., 2009. Eddy activity in the four major upwelling systems from satellite altimetry (1992–2007). *Progress in Oceanography*, *83*(1-4), pp.117-123.

Chavez, F.P. and Messié, M., 2009. A comparison of eastern boundary upwelling ecosystems. *Progress in Oceanography*, *83*(1-4), pp.80-96.

Chavez, F.P. and Messié, M., 2009. A comparison of eastern boundary upwelling ecosystems. *Progress in Oceanography*, *83*(1-4), pp.80-96.

Chhak, K. and Di Lorenzo, E., 2007. Decadal variations in the California Current upwelling cells. *Geophysical Research Letters*, *34*(14).

Cole, D., 1999. *Franz Boas: the early years, 1859-1906*. Douglas & McIntyre.

Cowtan, K., Rohde, R. and Hausfather, Z., 2018. Evaluating biases in sea surface temperature records using coastal weather stations. *Quarterly Journal of the Royal Meteorological Society*, *144*(712), pp.670-681.

Cury, P. and Shannon, L., 2004. Regime shifts in upwelling ecosystems: observed changes and possible mechanisms in the northern and southern Benguela. *Progress in Oceanography*, *60*(2-4), pp.223-243.

Dewitte, B., Vazquez-Cuervo, J., Goubanova, K., Illig, S., Takahashi, K., Cambon, G., Purca, S., Correa, D., Gutiérrez, D., Sifeddine, A. and Ortlieb, L., 2012. Change in El Nino flavours over 1958–2008: Implications for the long-term trend of the upwelling off Peru. *Deep Sea Research Part II: Topical Studies in Oceanography*, *77*, pp.143-156.

Diffenbaugh, N.S., Snyder, M.A. and Sloan, L.C., 2004. Could CO2-induced land-cover feedbacks alter near-shore upwelling regimes?. *Proceedings of the National Academy of Sciences*, *101*(1), pp.27-32.

Di Lorenzo, E., Schneider, N., Cobb, K.M., Franks, P.J.S., Chhak, K., Miller, A.J., McWilliams, J.C., Bograd, S.J., Arango, H., Curchitser, E. and Powell, T.M., 2008. North Pacific Gyre Oscillation links ocean climate and ecosystem change. *Geophysical Research Letters*, *35*(8).

Doney, S.C., Ruckelshaus, M., Duffy, J.E., Barry, J.P., Chan, F., English, C.A., Galindo, H.M., Grebmeier, J.M., Hollowed, A.B., Knowlton, N. and Polovina, J., 2011. Climate change impacts on marine ecosystems.

Dong, B., Sutton, R.T. and Scaife, A.A., 2006. Multidecadal modulation of El Niño–Southern Oscillation (ENSO) variance by Atlantic Ocean sea surface temperatures. *Geophysical Research Letters*, *33*(8).

Donlon, C. J., Martin, M., Stark, J., Roberts-Jones, J., Fiedler, E. and Wimmer, W. (2012). The operational sea surface temperature and sea ice analysis (OSTIA) system. *Remote Sensing of Environment*, *116*, pp.140-158.

Dorman, C.E. and Winant, C.D., 2000. The structure and variability of the marine atmosphere around the Santa Barbara Channel. *Monthly Weather Review*, *128*(2), pp.261-282.

Dufois, F., Penven, P., Whittle, C.P. and Veitch, J., 2012. On the warm nearshore bias in Pathfinder monthly SST products over Eastern Boundary Upwelling Systems. *Ocean Modelling*, *47*, pp.113-118.

Echevin, V., Albert, A., Lévy, M., Graco, M., Aumont, O., Piétri, A. and Garric, G., 2014. Intraseasonal variability of nearshore productivity in the Northern Humboldt Current System: The role of coastal trapped waves. *Continental Shelf Research*, *73*, pp.14-30.

Escribano, R., Daneri, G., Farías, L., Gallardo, V.A., González, H.E., Gutiérrez, D., Lange, C.B., Morales, C.E., Pizarro, O., Ulloa, O. and Braun, M., 2004. Biological and chemical consequences of the 1997–1998 El Niño in the Chilean coastal upwelling system: a synthesis. *Deep Sea Research Part II: Topical Studies in Oceanography*, *51*(20-21), pp.2389-2411.

Espinoza‐Morriberón, D., Echevin, V., Colas, F., Tam, J., Ledesma, J., Vásquez, L. and Graco, M., 2017. Impacts of E l N iño events on the P eruvian upwelling system productivity. *Journal of Geophysical Research: Oceans*, *122*(7), pp.5423-5444.

Fennel, W., 1999. Theory of the Benguela upwelling system. *Journal of Physical Oceanography*, *29*(2), pp.177-190.

Fielding, P. J. and Davis, C. L. (1989). Carbon and nitrogen resources available to kelp bed filter feeders in an upwelling environment. *Marine Ecology Progress Series*, pp.181-189.

Florenchie, P., Reason, C.J.C., Lutjeharms, J.R.E., Rouault, M., Roy, C. and Masson, S., 2004. Evolution of interannual warm and cold events in the southeast Atlantic Ocean. *Journal of Climate*, *17*(12), pp.2318-2334.

Fréon, P., Arístegui, J., Bertrand, A., Crawford, R.J., Field, J.C., Gibbons, M.J., Tam, J., Hutchings, L., Masski, H., Mullon, C. and Ramdani, M., 2009. Functional group biodiversity in Eastern Boundary Upwelling Ecosystems questions the wasp-waist trophic structure. *Progress in Oceanography*, *83*(1-4), pp.97-106.

García‐Reyes, M. and Largier, J., 2010. Observations of increased wind‐driven coastal upwelling off central California. *Journal of Geophysical Research: Oceans*, *115*(C4).

García-Reyes, M., Sydeman, W.J., Schoeman, D.S., Rykaczewski, R.R., Black, B.A., Smit, A.J. and Bograd, S.J., 2015. Under pressure: climate change, upwelling, and eastern boundary upwelling ecosystems. *Frontiers in Marine Science*, *2*, p.109.

Garreaud, R.D. and Falvey, M., 2009. The coastal winds off western subtropical South America in future climate scenarios. *International Journal of Climatology: A Journal of the Royal Meteorological Society*, *29*(4), pp.543-554.

Gillett, N.P., Fyfe, J.C. and Parker, D.E., 2013. Attribution of observed sea level pressure trends to greenhouse gas, aerosol, and ozone changes. *Geophysical Research Letters*, *40*(10), pp.2302-2306.

Graco, M.I., Purca, S., Dewitte, B., Castro, C.G., Morón, O., Ledesma, J., Flores, G. and Gutiérrez, D., 2017. The OMZ and nutrient features as a signature of interannual and low-frequency variability in the Peruvian upwelling system.

Guastella, L.A., 1992. Sea surface heat exchange at St Helena Bay and implications for the southern Benguela upwelling system. *South African Journal of Marine Science*, *12*(1), pp.61-70.

Gruber, N., Lachkar, Z., Frenzel, H., Marchesiello, P., Münnich, M., McWilliams, J.C., Nagai, T. and Plattner, G.K., 2011. Eddy-induced reduction of biological production in eastern boundary upwelling systems. *Nature geoscience*, *4*(11), pp.787-792.

Griffies, S.M., Yin, J., Durack, P.J., Goddard, P., Bates, S.C., Behrens, E., Bentsen, M., Bi, D., Biastoch, A., Böning, C.W. and Bozec, A., 2014. An assessment of global and regional sea level for years 1993–2007 in a suite of interannual CORE-II simulations. *Ocean Modelling*, *78*, pp.35-89.

Gutknecht, E., Dadou, I., Marchesiello, P., Cambon, G., Le Vu, B., Sudre, J., Garçon, V., Machu, E., Rixen, T., Kock, A. and Flohr, A., 2013. Nitrogen transfers off Walvis Bay: a 3-D coupled physical/biogeochemical modeling approach in the Namibian upwelling system. *Biogeosciences*, *10*(6), pp.4117-4135.

Haack, T., Chelton, D., Pullen, J., Doyle, J.D. and Schlax, M., 2008. Summertime influence of SST on surface wind stress off the US West Coast from the US Navy COAMPS model. *Journal of physical oceanography*, *38*(11), pp.2414-2437.

Hagen, E., 2009. Atlantic Exploration and Climate. *Selected Contributions on Results of Climate Research in East Germany*, pp.80-95.

Halpern, D., 2002. Offshore Ekman transport and Ekman pumping off Peru during the 1997–1998 El Nino. *Geophysical Research Letters*, *29*(5), pp.19-1.

Harlass, J., Latif, M. and Park, W. (2015). Improving climate model simulation of tropical Atlantic sea surface temperature: The importance of enhanced vertical atmosphere model resolution. *Geophysical Research Letters*, *42*(7), pp.2401-2408.

Harley, C.D., Randall Hughes, A., Hultgren, K.M., Miner, B.G., Sorte, C.J., Thornber, C.S., Rodriguez, L.F., Tomanek, L. and Williams, S.L., 2006. The impacts of climate change in coastal marine systems. *Ecology letters*, *9*(2), pp.228-241.

Hausfather, Z., Cowtan, K., Menne, M.J. and Williams Jr, C.N., 2016. Evaluating the impact of US historical climatology network homogenization using the US climate reference network. *Geophysical Research Letters*, *43*(4), pp.1695-1701.

Hoegh-Guldberg, O. and Bruno, J.F., 2010. The impact of climate change on the world's marine ecosystems. *Science*, *328*(5985), pp.1523-1528.

Hutchings, L., Van der Lingen, C. D., Shannon, L. J., Crawford, R. J. M., Verheye, H. M. S., Bartholomae, C. H., Van der Plas, A. K., Louw, D., Kreiner, A., Ostrowski, M. and Fidel, Q. (2009). The Benguela Current: An ecosystem of four components. *Progress in Oceanography*, *83*(1-4), pp.15-32.

Huyer, A., 1983. Coastal upwelling in the California Current system. *Progress in oceanography*, *12*(3), pp.259-284.

Hsieh, W.W and Boer, G.J. (1992). Global climate change and ocean upwelling. *Fisheries Oceanography*, *1*(4), pp.333-338.

Jacox, M.G., Fiechter, J., Moore, A.M. and Edwards, C.A., 2015. ENSO and the C alifornia C urrent coastal upwelling response. *Journal of Geophysical Research: Oceans*, *120*(3), pp.1691-1702.

Jakoboski, J., Todd, R.E., Owens, W.B., Karnauskas, K.B. and Rudnick, D.L., 2020. Bifurcation and upwelling of the equatorial undercurrent west of the Galapagos archipelago. *Journal of Physical Oceanography*, *50*(4), pp.887-905.

Jury, M. R. (1980). Characteristics of summer wind field and air sea interaction over the Cape Peninsula upwelling regions. M.Sc. Thesis. University of Cape Town, South Africa.

Kennedy, J.J., Rayner, N.A., Smith, R.O., Parker, D.E. and Saunby, M., 2011. Reassessing biases and other uncertainties in sea surface temperature observations measured in situ since 1850: 1. Measurement and sampling uncertainties. *Journal of Geophysical Research: Atmospheres*, *116*(D14).

Kessler, W.S., 2002. Is ENSO a cycle or a series of events?. *Geophysical Research Letters*, *29*(23), pp.40-1.

Kilpatrick, K.A., Podesta, G.P. and Evans, R., 2001. Overview of the NOAA/NASA advanced very high resolution radiometer Pathfinder algorithm for sea surface temperature and associated matchup database. *Journal of Geophysical Research: Oceans*, *106*(C5), pp.9179-9197.

Klein, S.A., Soden, B.J. and Lau, N.C., 1999. Remote sea surface temperature variations during ENSO: Evidence for a tropical atmospheric bridge. *Journal of climate*, *12*(4), pp.917-932.

Lau, N.C., 1997. Interactions between global SST anomalies and the midlatitude atmospheric circulation. *Bulletin of the American Meteorological Society*, *78*(1), pp.21-34.

Li, A., Bo, Y., Zhu, Y., Guo, P., Bi, J. and He, Y. (2013). Blending multi-resolution satellite sea surface temperature (SST) products using Bayesian maximum entropy method. *Remote sensing of environment*, *135*, pp.52-63.

Lima, F. P. and Wethey, D. S. (2012). Three decades of high-resolution coastal sea surface temperatures reveal more than warming. *Nature communications*, *3*(1), pp.1-13.

Lu, F., Hu, H., Sun, W., Zhu, J., Liu, G., Zhou, W., Zhang, Q., Shi, P., Liu, X., Wu, X. and Zhang, L., 2018. Effects of national ecological restoration projects on carbon sequestration in China from 2001 to 2010. *Proceedings of the National Academy of Sciences*, *115*(16), pp.4039-4044.

Mead, A., Griffiths, C. L., Branch, G. M., McQuaid, C. D., Blamey, L. K., Bolton, J. J., Anderson, R. J., Dufois, F., Rouault, M., Froneman, P. W. and Whitfield, A. K. (2013). Human-mediated drivers of change—impacts on coastal ecosystems and marine biota of South Africa. *African Journal of Marine Science*, *35*(3), pp.403-425.

Menne, M.J., Williams Jr, C.N. and Vose, R.S., 2009. The US Historical Climatology Network monthly temperature data, version 2. *Bulletin of the American Meteorological Society*, *90*(7), pp.993-1008.

Mesias, J. M., Bisagni, J. J. and Brunner, A. M. (2007). A high-resolution satellite-derived sea surface temperature climatology for the western North Atlantic Ocean. *Continental Shelf Research*, *27*(2), pp.191-207.

Messié, M., Ledesma, J., Kolber, D.D., Michisaki, R.P., Foley, D.G. and Chavez, F.P., 2009. Potential new production estimates in four eastern boundary upwelling ecosystems. *Progress in Oceanography*, *83*(1-4), pp.151-158.

Minnett, P. J. (1991). Consequences of sea surface temperature variability on the validation and applications of satellite measurements. *Journal of Geophysical Research: Oceans*, *96*(C10), pp.18475-18489.

Morales, C.E., Hormazábal, S.E. and Blanco, J., 1999. Interannual variability in the mesoscale distribution of the depth of the upper boundary of the oxygen minimum layer off northern Chile (18–24S): Implications for the pelagic system and biogeochemical cycling. Journal of Marine Research, 57(6), pp.909-932.

Montecino, V.I.V.I.A.N., RUTLLANT, J. and SALINAS, S., 2005. Coastal ocean circulation off western South America. *The Global Coastal Ocean-Regional Studies and Syntheses*, *11*, p.273.

Montecino, V. and Lange, C.B., 2009. The Humboldt Current System: Ecosystem components and processes, fisheries, and sediment studies. *Progress in Oceanography*, *83*(1-4), pp.65-79.

Morales, C.E., Hormazábal, S.E. and Blanco, J., 1999. Interannual variability in the mesoscale distribution of the depth of the upper boundary of the oxygen minimum layer off northern Chile (18–24S): Implications for the pelagic system and biogeochemical cycling. *Journal of Marine Research*, *57*(6), pp.909-932.

Mote, P. W. and Mantua, N. J. (2002). Coastal upwelling in a warmer future. *Geophysical research letters*, *29*(23), pp.53-1.

Mote, P.W. and Salathé, E.P., 2010. Future climate in the Pacific Northwest. *Climatic change*, *102*(1-2), pp.29-50.

Murawski, S. A. (1993). Climate change and marine fish distributions: forecasting from historical analogy. *Transactions of the American Fisheries Society*, *122*(5), pp.647-658.

Narayan, N., 2010. Interactive comment on "Trends in coastal upwelling intensity during the late 20th century" by N. Narayan et al.

Nelson, G. and Hutchings, L., 1983. The Benguela upwelling area. *Progress in Oceanography*, *12*(3), pp.333-356.

Pardo, P.C., Padín, X.A., Gilcoto, M., Farina-Busto, L. and Pérez, F.F., 2011. Evolution of upwelling systems coupled to the long-term variability in sea surface temperature and Ekman transport. *Climate Research*, *48*(2-3), pp.231-246.

Parker, D.E., Folland, C.K. and Jackson, M., 1995. Marine surface temperature: observed variations and data requirements. *Climatic Change*, *31*(2-4), pp.559-600.

Pauly, D. and Christensen, V., 1995. Primary production required to sustain global fisheries. Nature, 374(6519), pp.255-257.

Pauly, D. and Christensen, V., 1995. Primary production required to sustain global fisheries. *Nature*, *374*(6519), pp.255-257.

Pegliasco, C., Chaigneau, A. and Morrow, R., 2015. Main eddy vertical structures observed in the four major Eastern Boundary Upwelling Systems. *Journal of Geophysical Research: Oceans*, *120*(9), pp.6008-6033.

Pelegrí, J.L. and Peña-Izquierdo, J., 2015. Inorganic nutrients and dissolved oxygen in the Canary Current Large Marine Ecosystem.

Peterson, W.T. and Schwing, F.B., 2003. A new climate regime in northeast Pacific ecosystems. *Geophysical research letters*, *30*(17).

Perlin, N., Samelson, R.M. and Chelton, D.B., 2004. Scatterometer and model wind and wind stress in the Oregon–northern California coastal zone. *Monthly Weather Review*, *132*(8), pp.2110-2129.

Perlin, N., Skyllingstad, E.D. and Samelson, R.M., 2010. Coastal Atmospheric Circulation around a Cape and its Response to Wind-Driven Upwelling Studied Using a Coupled Ocean-Atmosphere Model.

Perlin, N., Skyllingstad, E.D. and Samelson, R.M., 2011. Coastal atmospheric circulation around an idealized cape during wind-driven upwelling studied from a coupled ocean–atmosphere model. *Monthly Weather Review*, *139*(3), pp.809-829.

Rahmstorf, S., 2002. Ocean circulation and climate during the past 120,000 years. *Nature*, *419*(6903), pp.207-214.

Rasmusson, E.M. and Carpenter, T.H., 1982. Variations in tropical sea surface temperature and surface wind fields associated with the Southern Oscillation/El Niño. *Monthly Weather Review*, *110*(5), pp.354-384.

Rayner, N. A., Brohan, P., Parker, D. E., Folland, C. K., Kennedy, J. J., Vanicek, M., Ansell, T. J. and Tett, S. F. B. (2006). Improved analyses of changes and uncertainties in sea surface temperature measured in situ since the mid-nineteenth century: The HadSST2 dataset. *Journal of Climate*, *19*(3), pp.446-469.

Reynolds, R. W. and Smith, T. M. (1994). Improved global sea surface temperature analyses using optimum interpolation. *Journal of climate*, *7*(6), pp.929-948.

Reynolds, R. W. and Smith, T. M. (1995). A high-resolution global sea surface temperature climatology. *Journal of Climate*, *8*(6), pp.1571-1583.

Reynolds, R. W., Rayner, N. A., Smith, T. M., Stokes, D. C. and Wang, W. (2002). An improved in situ and satellite SST analysis for climate. *Journal of climate*, *15*(13), pp.1609-1625.

Reynolds, R. W. and Chelton, D. B. (2010). Comparisons of daily sea surface temperature analyses for 2007–08. *Journal of climate*, *23*(13), pp.3545-3562.

Reynolds, R. W., Chelton, D. B., Roberts-Jones, J., Martin, M. J., Menemenlis, D. and Merchant, C. J. (2013). Objective determination of feature resolution in two sea surface temperature analyses. *Journal of climate*, *26*(8), pp.2514-2533.

Ricciardulli, L. and Wentz, F. J. (2004). Uncertainties in sea surface temperature retrievals from space: Comparison of microwave and infrared observations from TRMM. *Journal of Geophysical Research: Oceans*, *109*(C12).

Rimbu, N., Lohmann, G., Kim, J.H., Arz, H.W. and Schneider, R., 2003. Arctic/North Atlantic Oscillation signature in Holocene sea surface temperature trends as obtained from alkenone data. *Geophysical research letters*, *30*(6).

Risien, C.M., Reason, C.J.C., Shillington, F.A. and Chelton, D.B., 2004. Variability in satellite winds over the Benguela upwelling system during 1999–2000. *Journal of Geophysical Research: Oceans*, *109*(C3).

Robinson, I. S., Wells, N. C. and Charnock, H. (1984). The sea surface thermal boundary layer and its relevance to the measurement of sea surface temperature by airborne and spaceborne radiometers. *International Journal of Remote Sensing*, *5*(1), pp.19-45.

Roemmich, D. and McGowan, J., 1995. Climatic warming and the decline of zooplankton in the California Current. *Science*, *267*(5202), pp.1324-1326.

Rossi, V., 2010. *Influence of mesoscale physical processes on planktonic ecosystems in the regional ocean: application to the Eastern Boundary Upwelling Systems* (Doctoral dissertation).

Rouault, M., Florenchie, P., Fauchereau, N. and Reason, C.J., 2003. South East tropical Atlantic warm events and southern African rainfall. *Geophysical Research Letters*, *30*(5).

Rouault, M., Pohl, B. and Penven, P., 2010. Coastal oceanic climate change and variability from 1982 to 2009 around South Africa. *African Journal of Marine Science*, *32*(2), pp.237-246.

Rykaczewski, R.R., Dunne, J.P., Sydeman, W.J., García‐Reyes, M., Black, B.A. and Bograd, S.J., 2015. Poleward displacement of coastal upwelling‐favorable winds in the ocean's eastern boundary currents through the 21st century. *Geophysical Research Letters*, *42*(15), pp.6424-6431.

Samanta, D., Karnauskas, K.B. and Goodkin, N.F., 2019. Tropical Pacific SST and ITCZ biases in climate models: Double trouble for future rainfall projections?. *Geophysical Research Letters*, *46*(4), pp.2242-2252.

Santos, F., Gomez-Gesteira, M., Decastro, M. and Alvarez, I., 2012. Differences in coastal and oceanic SST trends due to the strengthening of coastal upwelling along the Benguela current system. *Continental Shelf Research*, *34*, pp.79-86.

Seabra, R., Varela, R., Santos, A.M., Gómez-Gesteira, M., Meneghesso, C., Wethey, D.S. and Lima, F.P., 2019. Reduced nearshore warming associated with eastern boundary upwelling systems. *Frontiers in Marine Science*, *6*, p.104.

Schlegel, R. W. and Smit, A. J. (2016). Climate change in coastal waters: time series properties affecting trend estimation. *Journal of Climate*, *29*(24), pp.9113-9124.
Schlegel, R. W., Oliver, E. C., Perkins-Kirkpatrick, S., Kruger, A. and Smit, A. J. (2017). Predominant atmospheric and oceanic patterns during coastal marine heatwaves. *Frontiers in Marine Science*, *4*, p.323.

Schlegel, R.W. and Smit, A.J., 2018. heatwaveR: a central algorithm for the detection of heatwaves and cold-spells. *Journal of Open Source Software*, *3*(27), p.821.

Schultz, O.J., 2010. *Belonging to the West Coast: an ethnography of St Helena Bay in the context of marine resource scarcity* (Doctoral dissertation, University of Cape Town).

Scoccimarro, E., Gualdi, S., Bellucci, A., Sanna, A., Giuseppe Fogli, P., Manzini, E., Vichi, M., Oddo, P. and Navarra, A., 2011. Effects of tropical cyclones on ocean heat transport in a high-resolution coupled general circulation model. *Journal of Climate*, *24*(16), pp.4368-4384.

Servain, J., Picaut, J. and Busalacchi, A.J., 1985. Interannual and seasonal variability of the tropical Atlantic Ocean depicted by sixteen years of sea-surface temperature and wind stress. In *Elsevier oceanography series* (Vol. 40, pp. 211-237). Elsevier.

Shaffer, G., Pizarro, O., Djurfeldt, L., Salinas, S. and Rutllant, J., 1997. Circulation and low-frequency variability near the Chilean coast: Remotely forced fluctuations during the 1991–92 El Nino. *Journal of Physical Oceanography*, *27*(2), pp.217-235.

Shannon, L.V., 1985. The Benguela ecosystem. I: Evolution of the Benguela physical features and processes. Oceanography and Marine Biology, 23, pp.105-182.

Shannon, L.V., Boyd, A.J., Brundrit, G.B. and Taunton-Clark, J., 1986. On the existence of an El Niño-type phenomenon in the Benguela system. *Journal of marine Research*, *44*(3), pp.495-520.

Smith, T. M. and Reynolds, R. W. (1998). A high-resolution global sea surface temperature climatology for the 1961–90 base period. *Journal of Climate*, *11*(12), pp.3320-3323.

Smit, A. J., Roberts, M., Anderson, R. J., Dufois, F., Dudley, S. F., Bornman, T. G., Olbers, J. and Bolton, J. J. (2013). A coastal seawater temperature dataset for biogeographical studies: large biases between in situ and remotely-sensed data sets around the coast of South Africa. *PLoS One*, *8*(12).

Snyder, M.A., Sloan, L.C., Diffenbaugh, N.S. and Bell, J.L., 2003. Future climate change and upwelling in the California Current. *Geophysical Research Letters*, *30*(15).

Stenseth, N.C., Mysterud, A., Ottersen, G., Hurrell, J.W., Chan, K.S. and Lima, M., 2002. Ecological effects of climate fluctuations. *Science*, *297*(5585), pp.1292-1296.

Stander, G.H. and De Decker, A.H.B., 1969. *Some physical and biological aspects of an oceanographic anomaly off South West Africa in 1963*. Department of Commerce, Division of Fisheries.

Stocker, T.F., Qin, D., Plattner, G.K., Tignor, M., Allen, S.K., Boschung, J., Nauels, A., Xia, Y., Bex, V. and Midgley, P.M., 2013. Climate change 2013: The physical science basis. *Contribution of working group I to the fifth assessment report of the intergovernmental panel on climate change*, *1535*.

Sutton, R.T., Jewson, S.P. and Rowell, D.P., 2000. The elements of climate variability in the tropical Atlantic region. *Journal of Climate*, *13*(18), pp.3261-3284.

Sydeman, W.J., Santora, J.A., Thompson, S.A., Marinovic, B. and Lorenzo, E.D., 2013. Increasing variance in North Pacific climate relates to unprecedented ecosystem variability off California. *Global Change Biology*, *19*(6), pp.1662-1675.

Sydeman, W.J., García-Reyes, M., Schoeman, D.S., Rykaczewski, R.R., Thompson, S.A., Black, B.A. and Bograd, S.J., 2014. Climate change and wind intensification in coastal upwelling ecosystems. *Science*, *345*(6192), pp.77-80.

Sverdrup, H.U. and Allen, W.E., 1939. Distribution of diatoms in relation to the character of water masses and currents off southern California in 1938. *J. mar. Res*, *2*(2), pp.131-144.
Tang, DanLing, Dana R. Kester, Zhaoding Wang, Jiansheng Lian, and Hiroshi Kawamura. "AVHRR satellite remote sensing and shipboard measurements of the thermal plume from the Daya Bay, nuclear power station, China." *Remote Sensing of Environment* 84, no. 4 (2003): 506-515.

Tim, N., Zorita, E. and Hünicke, B., 2015. Decadal variability and trends of the Benguela upwelling system as simulated in a high-resolution ocean simulation. *Ocean Sci*, *11*(3), pp.483-502.

Timmermann, A., Oberhuber, J., Bacher, A., Esch, M., Latif, M. and Roeckner, E., 1999. Increased El Niño frequency in a climate model forced by future greenhouse warming. *Nature*, *398*(6729), pp.694-697.

Tittensor, D.P., Mora, C., Jetz, W., Lotze, H.K., Ricard, D., Berghe, E.V. and Worm, B., 2010. Global patterns and predictors of marine biodiversity across taxa. *Nature*, *466*(7310), pp.1098-1101.

Tyson, P.D. and Preston-Whyte, R.A., 2000. *Weather and climate of southern Africa*. Oxford University Press.

Ulloa, O., Escribano, R., Hormazabal, S., Quinones, R.A., González, R.R. and Ramos, M., 2001. Evolution and biological effects of the 1997–98 El Nino in the upwelling ecosystem off northern Chile. *Geophysical Research Letters*, *28*(8), pp.1591-1594.

Van Heerden, J. and Hurry, L., 1998. Southern Africa's weather patterns: An introductory guide. Collegium.

Vargas, G., Pantoja, S., Rutllant, J.A., Lange, C.B. and Ortlieb, L., 2007. Enhancement of coastal upwelling and interdecadal ENSO‐like variability in the Peru‐Chile Current since late 19th century. *Geophysical Research Letters*, *34*(13).

Walker, A., 2020. *Observed Trends of Coastal Upwelling in Eastern Boundary Upwelling Systems* (Doctoral dissertation, University of Colorado at Boulder).

Wang, W. and McPhaden, M.J., 2000. The surface-layer heat balance in the equatorial Pacific Ocean. Part II: Interannual variability. *Journal of Physical Oceanography*, *30*(11), pp.2989-3008.

Wang, X.L., Cai, X.D., Su, Z.E., Chen, M.C., Wu, D., Li, L., Liu, N.L., Lu, C.Y. and Pan, J.W., 2015. Quantum teleportation of multiple degrees of freedom of a single photon. *Nature*, *518*(7540), pp.516-519.

Whitfield, A.K., James, N.C., Lamberth, S.J., Adams, J.B., Perissinotto, R., Rajkaran, A. and Bornman, T.G., 2016. The role of pioneers as indicators of biogeographic range expansion caused by global change in southern African coastal waters. *Estuarine, Coastal and Shelf Science*, *172*, pp.138-153.

Wick, G. A., Emery, W. J. and Schluessel, P. (1992). A comprehensive comparison between satellite‐measured skin and multichannel sea surface temperature. *Journal of Geophysical Research: Oceans*, *97*(C4), pp.5569-5595.

Wycech, J.B., Gill, E., Rajagopalan, B., Marchitto Jr, T.M. and Molnar, P.H., 2020. Multiproxy Reduced‐Dimension Reconstruction of Pliocene Equatorial Pacific Sea Surface Temperatures. *Paleoceanography and Paleoclimatology*, *35*(1), p.e2019PA003685.

Zebiak, S.E., 1993. Air–sea interaction in the equatorial Atlantic region. *Journal of Climate*, *6*(8), pp.1567-1586.

Zhang, L., Han, W., Karnauskas, K.B., Meehl, G.A., Hu, A., Rosenbloom, N. and Shinoda, T., 2019. Indian Ocean warming trend reduces Pacific warming response to anthropogenic greenhouse gases: An interbasin thermostat mechanism. *Geophysical Research Letters*, *46*(19), pp.10882-10890.